AD-A143 456 BASIC PROBLEMS IN INP TECHNOLOGY(U) HUGHES RESEARCH LABS MALIBU CA K V VAIDYANATHAN ET AL. MAR 84 AFOSR-TR-84-0583 F49620-82-C-0040 1/1

UNCLASSIFIED F/G 20/12 NL

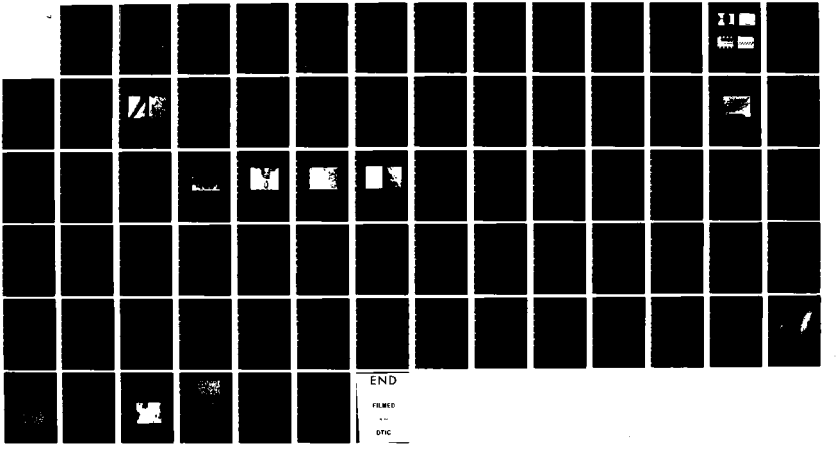

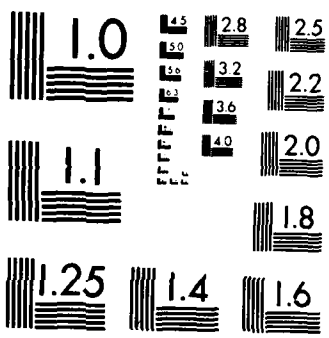

AFOSR-TR- 84-0583

(10)

BASIC PROBLEMS IN InP TECHNOLOGY

K.V. Vaidyanathan and H.L. Dunlap

Hughes Research Laboratories
3011 Malibu Canyon Road
Malibu, CA 90265

March 1984

F49620-82-C-0040
Final Report
16 November 1979 to 15 November 1980
28 February 1981 to 27 February 1982
1 April 1982 to 31 March 1983

AFOSR/NE
Director of Electronic and Material Science
Building 410
Bolling AFB, DC 20332

UNCLASSIFIED

SECURITY CLASSIFICATION OF THIS PAGE *(When Data Entered)*

REPORT DOCUMENTATION PAGE		READ INSTRUCTIONS BEFORE COMPLETING FORM
1. REPORT NUMBER **AFOSR-TR- 84-0583**	2. GOVT ACCESSION NO. AD-A143	3. RECIPIENT'S CATALOG NUMBER 456
4. TITLE *(and Subtitle)* BASIC PROBLEMS IN InP TECHNOLOGY		5. TYPE OF REPORT & PERIOD COVERED Final Report 16 Nov 79 thru 31 Mar 83
		6. PERFORMING ORG. REPORT NUMBER
7. AUTHOR(s) K.V. VAIDYANATHAN and H.L. DUNLAP		8. CONTRACT OR GRANT NUMBER(s) F49620-82-C-0040
9. PERFORMING ORGANIZATION NAME AND ADDRESS Hughes Research Laboratories 3011 Malibu Canyon Road Malibu, California 90265		10. PROGRAM ELEMENT, PROJECT, TASK AREA & WORK UNIT NUMBERS 61102F 2306 B1
11. CONTROLLING OFFICE NAME AND ADDRESS Air Force Office of Scientific Research Bolling AFB, DC 20332		12. REPORT DATE March 1984
		13. NUMBER OF PAGES 74
14. MONITORING AGENCY NAME & ADDRESS*(if different from Controlling Office)*		15. SECURITY CLASS. *(of this report)* Unclassified
		15a. DECLASSIFICATION/DOWNGRADING SCHEDULE

16. DISTRIBUTION STATEMENT *(of this Report)*

Approved for public release; unlimited distribution

17. DISTRIBUTION STATEMENT *(of the abstract entered in Block 20, if different from Report)*

18. SUPPLEMENTARY NOTES

19. KEY WORDS *(Continue on reverse side if necessary and identify by block number)*

InP Ion Implantation
Encapsulation
InP Electrical Properties
Rapid Thermal Annealing of InP
TEM Evaluation of InP
SIMS Study of InP
Redistribution of Dopants.

20. ABSTRACT *(Continue on reverse side if necessary and identify by block number)*

Procedures for evaluating the thermal stability of bulk semi-insulating InP have been developed. Determination of the concentrations in S.I. InP is a major analytical problem. Preliminary SIMS measurements show that significant redistribution of Fe can occur during high temperature processing.

DD FORM 1 JAN 73 1473 EDITION OF 1 NOV 65 IS OBSOLETE

UNCLASSIFIED

SECURITY CLASSIFICATION OF THIS PAGE *(When Data Entered)*

Severe degradation can occur in ion-implanted InP samples annealed with SiO_2 and encapsulated at temperatures of 750°C. The use of phosphosilicate glass dramatically reduces such surface degradation. Energy dispersive X-ray analysis (EDAX) shows that the loss of P at the surface is the cause of such degradation.

Beryllium is a well behaved acceptor dopant in InP. It can be electrically activated efficiently at as low an anneal temperature as 550°C. At high concentrations, Be diffuses rapidly. Silicon, selenium, tin and germanium are all well behaved donor dopants in InP. Implantation temperature has a profound effect on the subsequent electrical properties of the layer in selenium, tin and germanium implants. Transmission electron microscopic studies indicate that dislocation loops are the dominant defects present in ion-implanted and annealed InP. Preliminary studies indicate that high doping efficiencies can be achieved by annealing at high temperatures for periods < 1 minute.

TABLE OF CONTENTS

LIST OF ILLUSTRATIONS

SECTION 1

INTRODUCTION

A. ADVANTAGES OF InP

Both InP and the ternary InGaAs have electronic properties which make them attractive for high speed microwave and opto-electronic device applications. For example, both of these materials exhibit considerbly higher steady-state electron velocities at all values of electric field than does silicon. It is possible to grow $In_{0.53}$ $Ga_{0.47}As$ epitaxial layers lattice-matched to InP. At this composition of the ternary alloy, photodetectors capable of detecting 1.6 μm radiation have been fabricated. In this wavelength range low loss, low dispersion, radiation-resistant fibers are available, making these materials attractive for fiber optic applications. The unique properties of InP that make it attractive for high speed device applications are discussed below.

The electron velocity-electric field characteristics of silicon, gallium arsenide, and indium phosphide are shown in Figure 1. An inspection of this curve shows that at low fields (<0.6 V/μm) electrons in GaAs exhibit higher velocities than those in Si or InP. However, at higher fields (0.7 V to 2.3 V/μm) InP is clearly superior to either GaAs or Si. Also, the curves in Figure 1 represent steady-state values, and for them to be valid the following conditions must be satisfied: (1) the applied field should be constant over distances that are long compared to the optical phonon-scattering mean free path, and (2) the applied voltage across the region of constant field should be substantially greater than the energy difference between the direct and indirect condition band minima ($\Delta E_{\Gamma L}$). Violation of these conditions can lead to the phenomenon of "velocity overshoot." Such overshoot can result in carriers reaching substantially higher velocities than

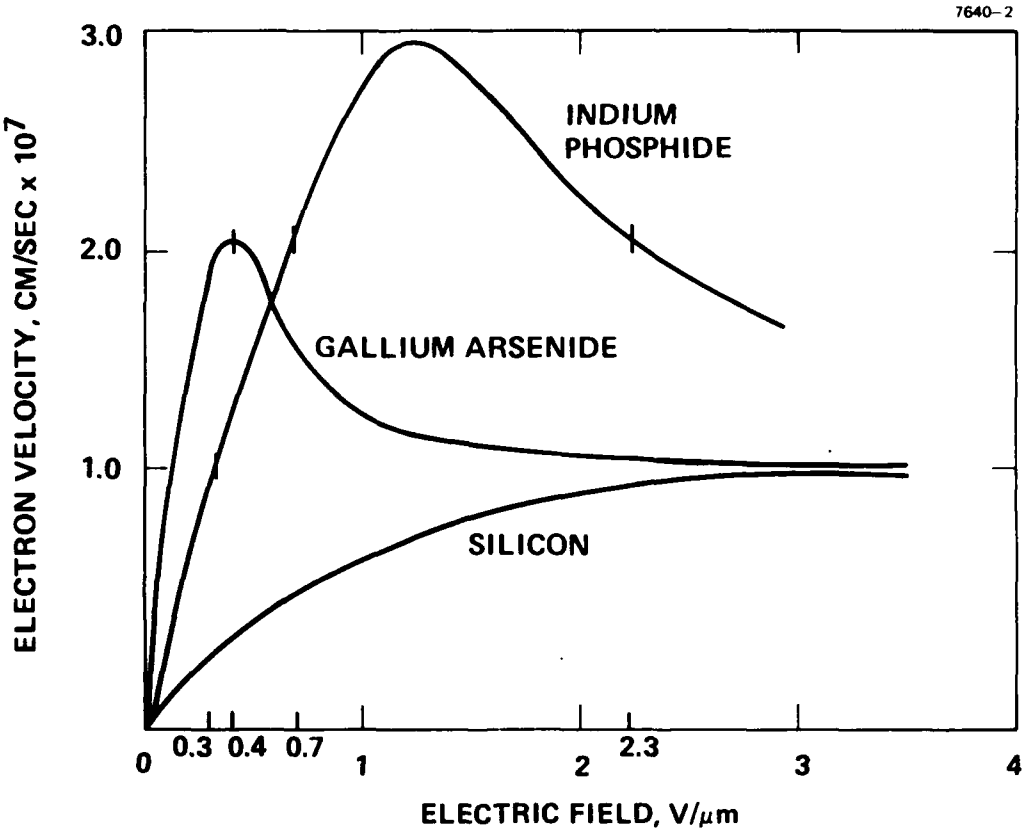

Figure 1. Electronic velocity versus electric field characteristics for Si, GaAs, and InP under steady-state conditions.

steady-state for a particular value of electric field. For practical GaAs devices, both conditions are satisfied for fields higher than 0.3 V/μm. In the case of InP, condition (2) may not be satisfied until a field of 0.7 V/μm is reached. Thus velocity overshoot effects may dominate in InP even at fields as high as 0.7 V/μm.

Another major advantage of InP is the ability to form a stable dielectric–semiconductor interface and the ability to fabricate metal insulator semiconductor field effect transistors (MISFETs). Such devices can sustain several volts of forward bias. In contrast, GaAs MESFET devices employing Schottky gates are limited to very small forward voltage swings. This feature relaxes the threshold voltage control requirements of individual devices for integrated circuit applications. We believe that this technology will be extremely useful in fabricating low power, high speed random access memories (RAMs).

As a result of this technology development program, we have established a reliable implantation and annealing process technology to form n^+ regions in InP. The results from this program have been used to fabricate discrete InP MISFET devices and integrated circuits employing such devices. The development and fabrication of devices and circuits were performed under Hughes internal research and development programs and an NOSC-sponsored IC program, respectively. The discrete MISFETs with implanted source and drain regions had a channel length of ~1.5 μm and a gate length of ~5 μm. The current-voltage characteristics of such a device are shown in Figure 2. Under an NOSC contract to demonstrate IC operation of MSI complexity employing InP MISFETs, we have demonstrated a 15-stage ring oscillator with implanted load resistors and enhancement mode transistors. These circuits operated with a gate delay of 120 psec. Typical results are shown in Figure 3. These encouraging results have been made possible because of the process technology developments achieved under this contract and our IR&D programs.

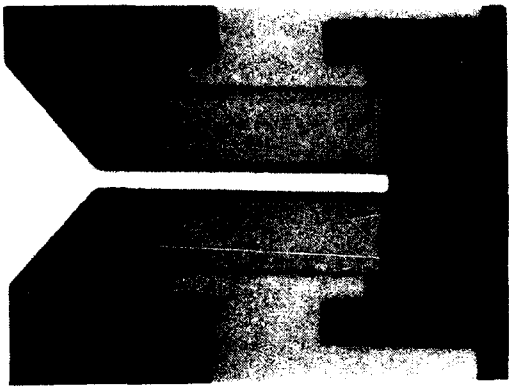

Figure 2(a).
Photograph of a planar InP MISFET with channel length of 1.5 μm.

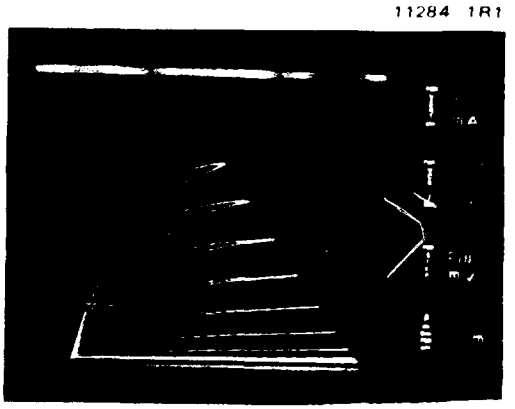

Figure 2(b).
I_D versus $_D$ characteristics for a InP E-MISFET.

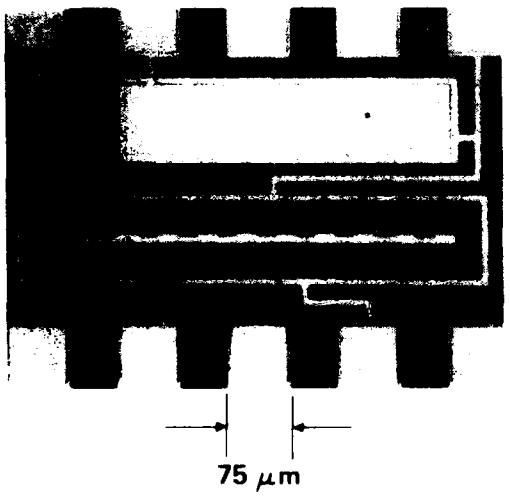

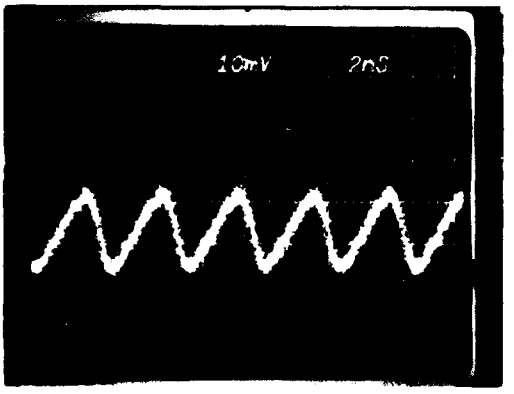

f_{out} = 277 MHz

t_{pd} = 120 ps

Figure 3. InP MISFET 15-stage ring oscillator.

The electronic properties of InGaAs also make it attractive for opto-electronic device applications. Photodetectors capable of operating at 1.6 μm can be fabricated on lattice-matched InGaAs layers grown on InP. This wavelength range is of great interest in fiber optic communications systems because of the availability of radiation resistant, low loss, low dispersion optical fibers. The mutually compatible InGaAs/InP, InGaAsP/InP system makes it possible to integrate sources, detectors, and high speed signal processing elements and thus develop intelligent opto-electronic integrated circuits.

In this report, we discuss the major areas of investigation carried out in the program.

- We have developed empirical procedures for evaluating the thermal stability of semi-insulating InP. In addition, we have developed techniques which can be used to determine quantitatively the iron content in semi-insulating InP. These include secondary ion mass spectrometry (SIMS), Zeeman atomic absorption (ZAA) spectroscopy, and electron paramagnetic resonance (EPR). The relative merits of each of these techniques will be discussed in more detail.

- We have investigated procedures for encapsulating ion-implanted InP with an appropriate dielectric during the annealing process. These include the evaluation of a plasma-enhanced deposited silicon nitride and phosphosilicate glass (PSG) as encapsulants.

- We have studied the electrical activation as well as atomic distribution of silicon, sulfur, carbon, selenium (donors) and beryllium (acceptor) implanted layers as a function of anneal parameters in InP. More detailed evaluations of the implanted dopants and defects present in the material will form the focal point for future investigations.

- We have performed preliminary investigations of the use of a rapid thermal annealling (RTA) technique to electrically activate ion-implanted dopants in InP.

- We have also investigated the microstructure in ion-implanted and annealed InP layers using transmission electron microscopy (TEM). This work was carried out under subcontract at the University of California, Berkeley.

This report discusses the progress in these areas in detail.

SECTION 2

EVALUATION OF BULK InP CRYSTALS

A. INTRODUCTION

The high vapor pressure of P over InP at a growth temperature of 1060°C makes it difficult to grow single crystal ingots of InP. These ingots are normally grown by the liquid encapsulated Czochralski (LEC) growth technique using boric oxide as the encapsulant. Ingots grown by the LEC technique from silica crucibles are normally n-type, with electron concentrations in the range of low- to mid 10^{16} cm^{-3}. The addition of deep level dopants such as Cr, Fe, and Co to the melt result in the growth of high resistivity InP crystals. Previous studies have shown that the solubility of Fe in InP is fairly high and results in the growth of semi-insulating crystals. Optical and electrical measurements of Fe-doped InP samples show that Fe is a deep acceptor in InP, with an ionization energy of ~0.65 eV. The availability of semi-insulating InP makes it an attractive candidate for high speed IC applications since it automatically provides the required device isolation. However, for such applications, it is also essential that the material remain semi-insulating after high temperature processing.

Two types of degradation can occur when InP wafers are subjected to high temperature processes. The first one occurs due to the loss of phosphorus from the surface, as shown in Figure 4(b). In this case, the samples were annealed in an ambient of flowing hydrogen at 730°C for 90 minutes. We have noticed this type of degradation in pulsed electron-beam-annealed InP samples which were performed in 1979 as a part of our IR&D program. Electrical evaluation of these E-beam-annealed samples revealed the presence of a highly conductive layer. Workers at RADC (East) using Rutherford backscattering analysis and electrical measurements have shown that at the conducting layers formed are due to loss of phophorus from the surface of InP.

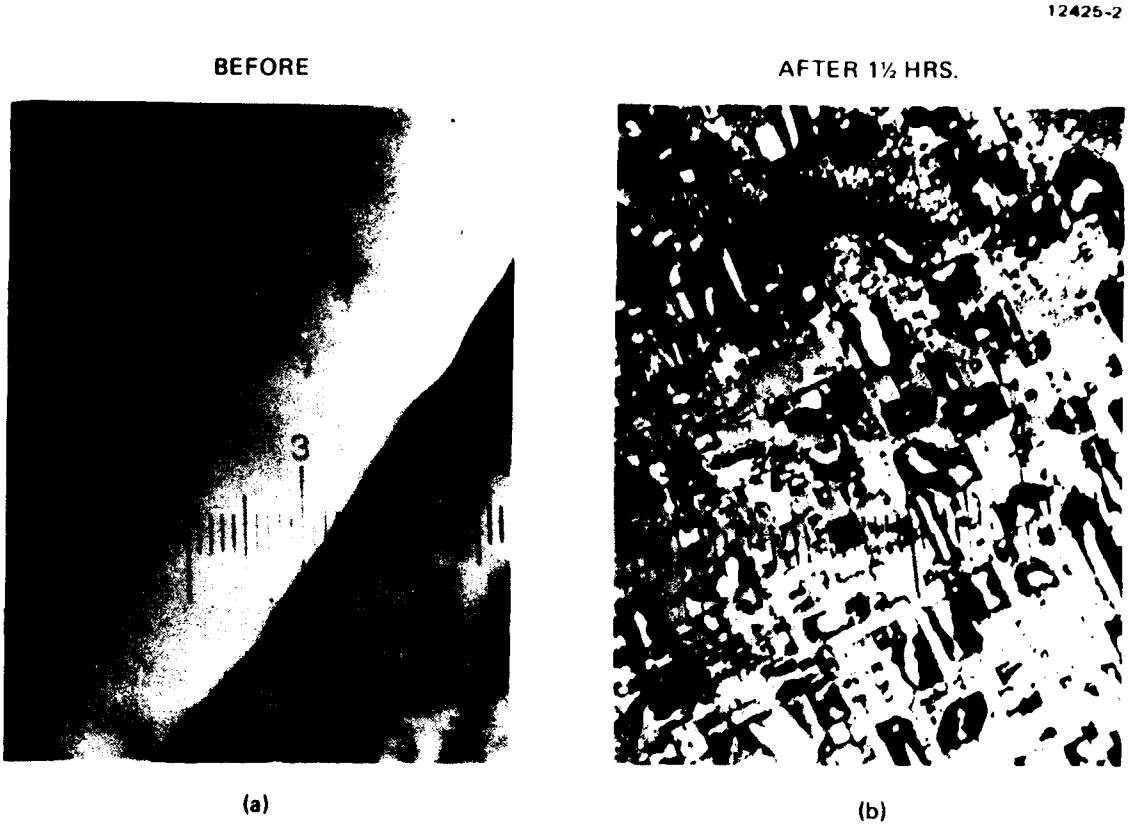

Figure 4. Decomposition of InP substrate at 730°C in H_2 ambient.

Another type of degradation is the surface conversion due to the redistribution of the deep level dopant during high temperature processing. A classic example of this type of problem is the redistribution of chromium in horizontal Bridgeman-grown Cr-doped semi-insulating GaAs. A detailed understanding of the mechanism responsible for Cr redistribution was made possible by using secondary ion mass spectrometry (SIMS) as an analytical tool. The first step to achieve this goal is to develop analytical techniques which can be used to determine the concentration of iron in InP crystals. Some of the techniques used to make such measurements under this program are discussed below.

Preparation of damage-free, smooth chem-mechanically polished InP surface is another major processing problem. We have demonstrated that the use of x-ray diffraction and damage revealing etches can be used to qualitatively evaluate the effectiveness of polishing procedures on InP. These details are also discussed below.

B. ESTIMATION OF Fe CONCENTRATION IN InP

In order to understand the conversion behavior observed in some Fe-doped InP crystals, it is necessary to know the concentration of Fe in the starting material accurately and to obtain the depth distribution of Fe in processed wafers.

Secondary ion mass spectrometry (SIMS) has been used to obtain the concentration dopants in several semiconductor systems including that of Cr in horizontal Bridgeman-grown S.I. GaAs. It has also been used to study the diffusion behavior of Cr in GaAs during high temperature processing. We have performed experiments to assess effectiveness of SIMS technique to determine the concentration of Fe in S.I. InP. The analyses were performed at Charles Evans and Associates. Severe technical problems encountered in estimating the Fe concentration in InP using SIMS and are discussed below in detail.

In the SIMS technique, a primary ion beam is used to sputter the sample. The sputtered ionized atoms are then mass analyzed. In order to analyze bulk doping levels in semiconductors, the sample is sputtered at a rapid rate. The rapid sputtering process improves signal-to-noise ratio. In order to analyze an element, one typically measures the number of counts at a mass corresponding to the most abundant isotope. In the case of Fe, the dominant isotope has a mass of 56. There are, however, several combinations of molecules which have the same atomic mass. For example, a singly ionized silicon molecule (Si^+_2) has a mass of 56. Si is a known dominant residual donor in InP and is present in large quantities. The presence of such interferences introduce considerable uncertainity in quantitative determination of Fe in InP. Under conditions used to perform bulk analysis of samples, a high sputtering rate (~1.5 μm/min) is used. To achieve such a high sputtering rate, an intense primary beam is used. The apertures and electrodes in the ion-source in normal Cameca Instruments are made of stainless steel. The use of intense beams can lead to undesired sputtering from apertures, thereby increasing the background counts at mass 56 thus distorting the analysis.

Samples from two ingots of InP grown by Sumitomo Electric Corporation, labeled A and B, were sent to Charles Evans and Associates for analysis. Both of the ingots did not exhibit any "conversion" behavior and passed our evaluation procedure described in Table 1. According to the information available from the vendor, wafers from crystal B were supposed to contain approximately 10 times more iron compared to wafers from ingot A. Data obtained from SIMS analysis of these samples are shown in Figure 5. Within the sensitivity of the technique, it appears that both these ingots contain the same amount of iron. This is an apparent contradiction. We have during, 1983, analyzed samples from six different ingots of InP using SIMS and other physiochemical analytical techniques.

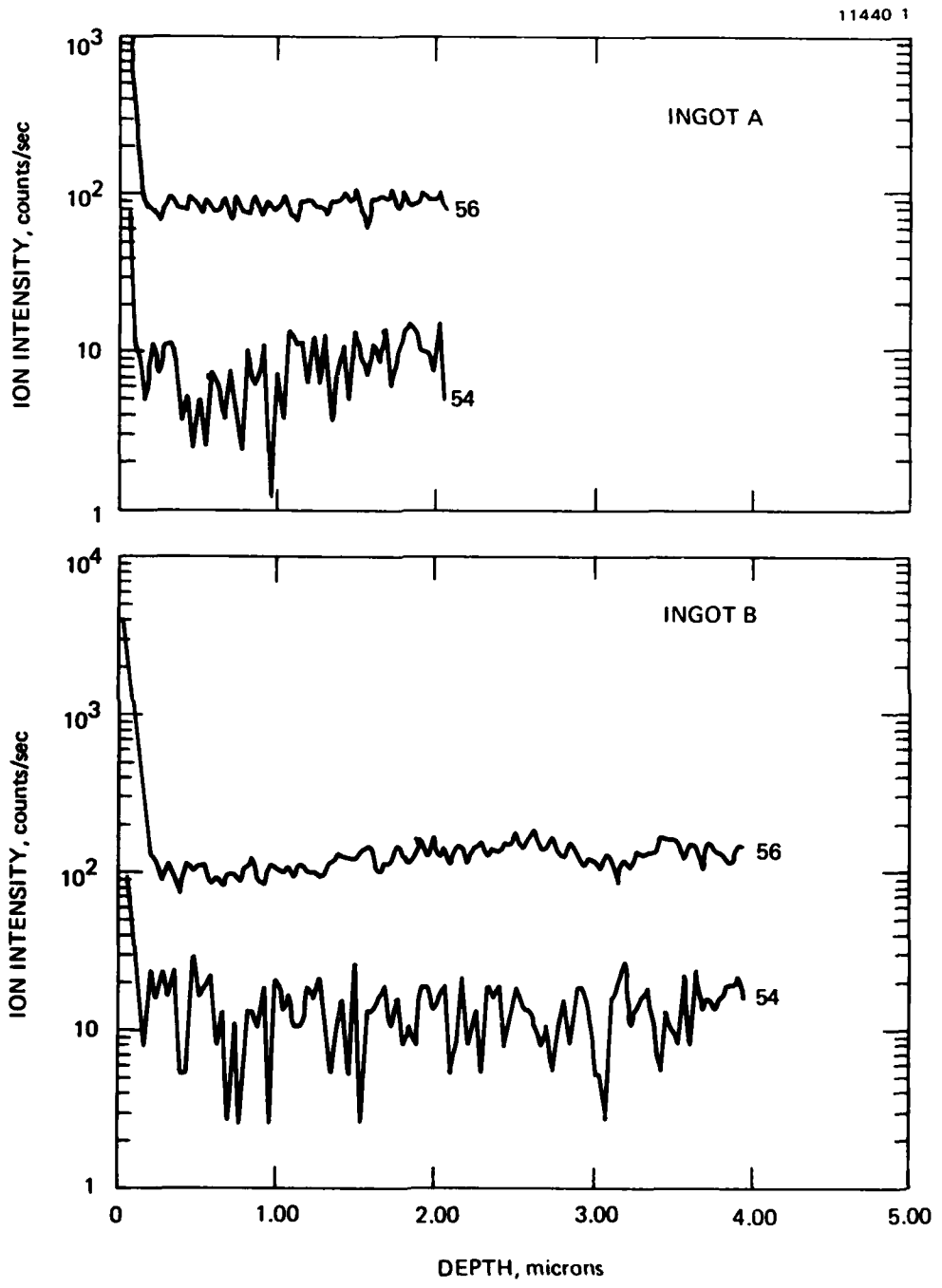

Figure 5. SIMS analysis of Fe concentration of InP ingot A and ingot B.

Table 1. Experimental Steps Involved in Evaluating InP Ingots

Measure resistivity of as-received sample. If $\rho > 10^7$ Ω-cm, proceed to next step.
Encapsulate the sample with ~1,500 Å PSG deposited at ~325°C.
Anneal encapsulated sample at 750°C for 30 min.
If the resistivity of annealed sample is greater than 10^6 Ω-cm, proceed to next step. If $\rho < 10^6$ Ω-cm, reject sample.
Implant silicon at 100 keV to a dose of 3×10^{12} cm^{-2}; encapsulate with PSG and anneal at 750°C for 30 min.
If the annealed sample exhibits >65% electrical activation, accept the ingot. If $\eta << 65\%$, reject ingot.

Zeeman Atomic Absorption (ZAA) spectrometry is a chemical analysis technique. A spectrophotometer developed by Dr. T. Hadeishi of Lawrence Berkeley Laboratory has been used to analyze the chromium and manganese content in GaAs by personnel at Hughes Research Laboratories. The technique utilizes the Zeeman effect on a resonant transition and can be used to automatically correct for background interference. This correction enhances the sensitivity of the technique in comparison with that of conventional atomic absorption spectroscopy.

The element to be analyzed (for example, Fe) is introduced in a hollow cathode arc discharge lamp confined in a uniform magnetic field of about 76 to 15 kG, as shown in Figure 6. The magnetic field induces Zeeman splitting of the characteristic emission lines. The emission line at the original wavelength is called the π-line, while the split lines are called σ-lines. In addition to splitting, the magnetic field also causes the lines to be polarized; the π-line is polarized in a plane parallel to

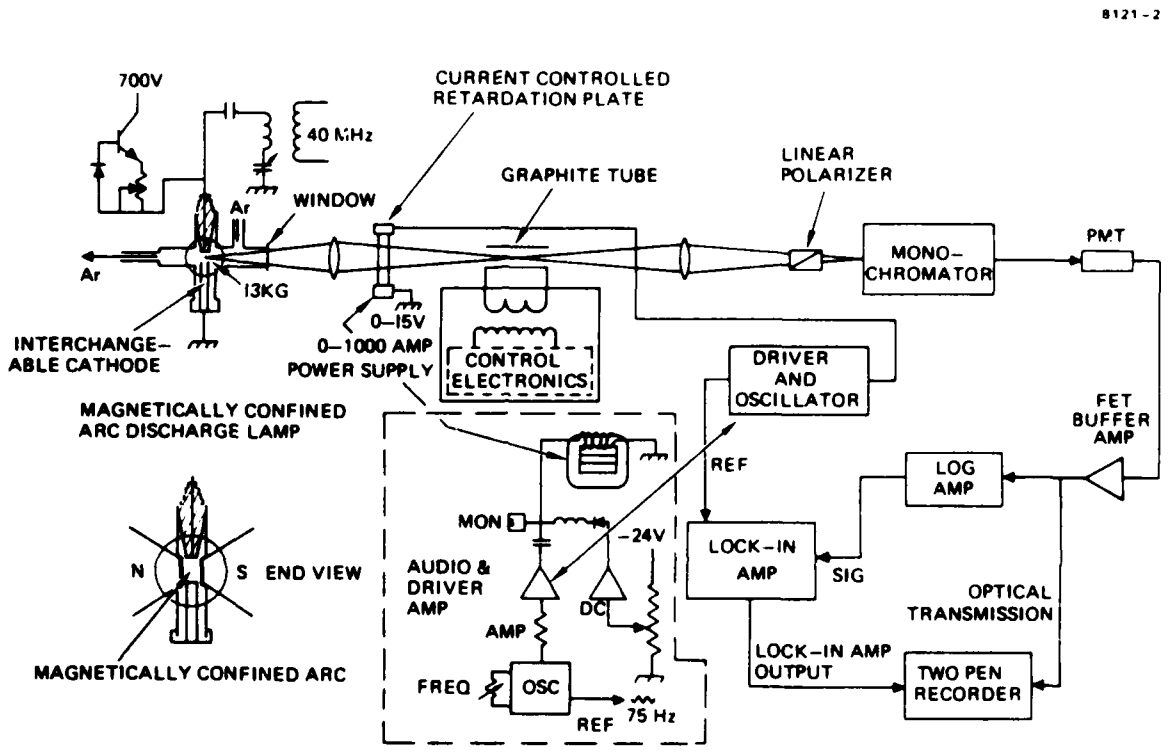

Figure 6. Schematic of Zeeman atomic absorption spectrometer.

the magnetic field, while the σ-lines are polarized in a plane perpendicular to the magnetic field. Thus, by using a suitable polarizer, either a π- or σ-beam can be selected. The sample to be analyzed (in this case, InP) is introduced into an atomizing furnace to be vaporized. The π- and σ-beams are passed through these vapors and the intensity of the transmitted emission measured. The π-beam is absorbed by the sample and by light scattering and broadband molecular absorption. The σ-lines, on the other hand, are absorbed only by broadband molecular absorption and light scattering. By suitably combining the π- and σ-beams, the background contribution due to light scattering and molecular absorption can be subtracted. This unique feature of the ZAA technique increases the element detection sensitivity as well as the selectivity. Preliminary results of ZAA measurements of Fe in InP appear encouraging. The emission (or absorption) associated with Fe occurs at 248.3 nm. When a pure Fe standard is used, the absorption line is quite narrow. In contrast, the iron signals from both InP and GaAs appear to be much broader.

We have used the ZAA technique to determine the concentration of Fe in six different ingots of InP. The results from this study are discussed in this section.

Another technique which can be used to determine the Fe concentration in InP is electron paramagnetic resonance (EPR) spectroscopy. Iron in one of its oxidation results (Fe^{2+}) is paramagnetic. The EPR technicque can therefore be used to determine the density of Fe present in InP which is in this oxidation state. The experimental process is relatively simple. It consists of mounting the sample to be analyzed in a microwave cavity in a magnetic field. The microwave excitation frequency is fixed and the magnetic field can be swept. The microwave absorption by the sample is monitored and at a particular value of the magnetic field (H), a resonance is observed when it satisfied the condition, $\omega_L = -qH/2mc$, where ω_L is the angular frequency of the microwave radiation and H is the magnetic

field. From a detailed analysis of the data, the concentration of Fe in InP in the paramagnetic state can be estimated.

Samples from six different InP ingots were supplied to code 5212, Naval Research Laboratory, Washington, D.C., at the request of Dr. G.L. Witt, the AFOSR program manager. At the time of writing this report, we have not received any quantitative data or representative spectra from NRL personnel. We have some qualitative data which is shown below in Table 2 .

Table 2. Concentration of Fe in InP Determined by ZAA SIMS, and EPR Techniques in Six Different Ingots

INGOT	Fe CONCENTRATION, cm^{-3}		
	ZAA	SIMS	EPR
MCP semi-insulating	~1.8×10^{16}	2.6×10^{16}	Fe presence detected
SUMITOMO semi-insulating	~4×10^{16}	~3×10^{16}	Fe presence detected
MRL Zn doped p-type ~1×10^{17} cm^{-3}	No Fe detected	No Fe detected	No Fe detected
MCP Zn-doped p-type ~1×10^{18} cm^{-3}	No Fe detected	No Fe detected	No Fe detected
MCP Si-doped p-type ~1×10^{18} cm^{-3}	No Fe detected	~ 2×10^{16}	Measurements could not be made — too lossy.
MCP Si-doped n-type 1×10^{16} cm^{-3}	No Fe	~1×10^{16}	No Fe detected

All of the above analytical techniques require Fe standards. For example, the standards for ZAA analysis are prepared by carefully weighting high purity Fe (a few ngms) and dissolving it completely in either HCl or HNO_3 and diluting the solution in water. The concentration of acidic aminia is sufficiently low that it does not interfere with the analysis.

In the case of SIMS, ion implanted standards can be used. For example, we have implanted F^+ at various energies 100 keV, 300 keV and 600 keV into InP to fluences of 1×10^{13} and 1×10^{14} cm^{-2}, and have used SIMS to obtain sensitivity factors. Under such conditions, a low sputtering rate is used, while during bulk analysis a very high sputtering rate is used to avoid spurious surface effects and to improve the signal-to-noise ratio. Since the analyzing conditions are different, it is possible that systematic errors can be introduced.

The data shown in Table 2 clearly demonstrates that there are problems associated with the determination of Fe concentration in InP using SIMS. High counts at mass 56 are seen in both semi-insulating and n-type samples. The true spectroscopic techniques (ZAA and EPR) are capable of determining the presence of Fe in InP. Quantitative detrermination still poses a problem. Also, these techniques (ZAA and EPR) do not provide any information on the depth distribution of Fe in InP.

The results from this study clearly demonstrate that quantitative determination of Fe in InP is a problem. Detailed investigations using a variety of analytical techniques are required for a viable solution.

C. SURFACE PREPARATION OF InP

In most FET devices the conduction betweeen the source and drain takes place in the near surface region. The presence of surface damage can reduce the surface carrier mobility, thus degrading device performance. Such degradation can be minimized

by preparing damage-free, smooth surfaces by appropriate procedures.

In this study we have concentrated on evaluating the surface perfection of InP samples by using chemical etching (to reveal subsurface damage) and by x-ray techniques. Material as received from two vendors was evaluated. The surface of the material from vendor A appeared specular mirror-like, and featureless. While the surface of material from vendor B appeared to exhibit an orange-peel-like appearance. On etching the surface of wafers from vendor A in a 5% solution of bromine in methanol, extensive surface pitting, indicative of the presence of surface damage in InP, was observed. Wafers from vendor B did not exhibit such surface features on etching. The micrograph ion Figure 12 illustrates the presence of surface damage in samples obtained from vendor A.

We have also evaluated the InP wafers by performing x-ray diffractometer studies using the double refractometer arrangement. CuK_{α} lines were used. The samples from vendor A exhibit extensive line broadening, while those from vendor B exhibit sharp featured lines. The line widths from sample B are normal and are instrument limited (as shown in Figure 13). Later, it was learned that the samples from vendor A were polished in a slurry of 0.05 μm zironium oxide, while vendor B used chem-mechanical polishing in a 5% solution of bromine in methanol as the last polishing procedure. These studies show that the chem-mechanically prepared surfaces can be damage free but are not, unfortunately, mirror-like and smooth. We have used x-ray diffraction and selective area electron diffraction (psuedo-kikuchi) techniques to ensure the crystallinity of the wafers.

12425-4

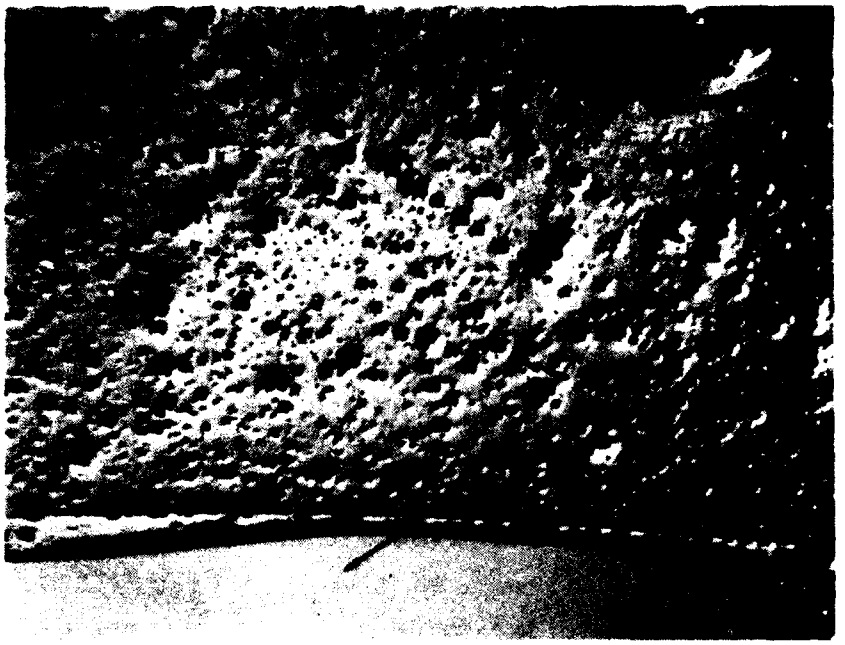

Figure 7. Micrograph showing extensive surface damage revealed by etching mechanically polished InP from Vendor A in a solution of 2% Br fin methanol for 1 min.

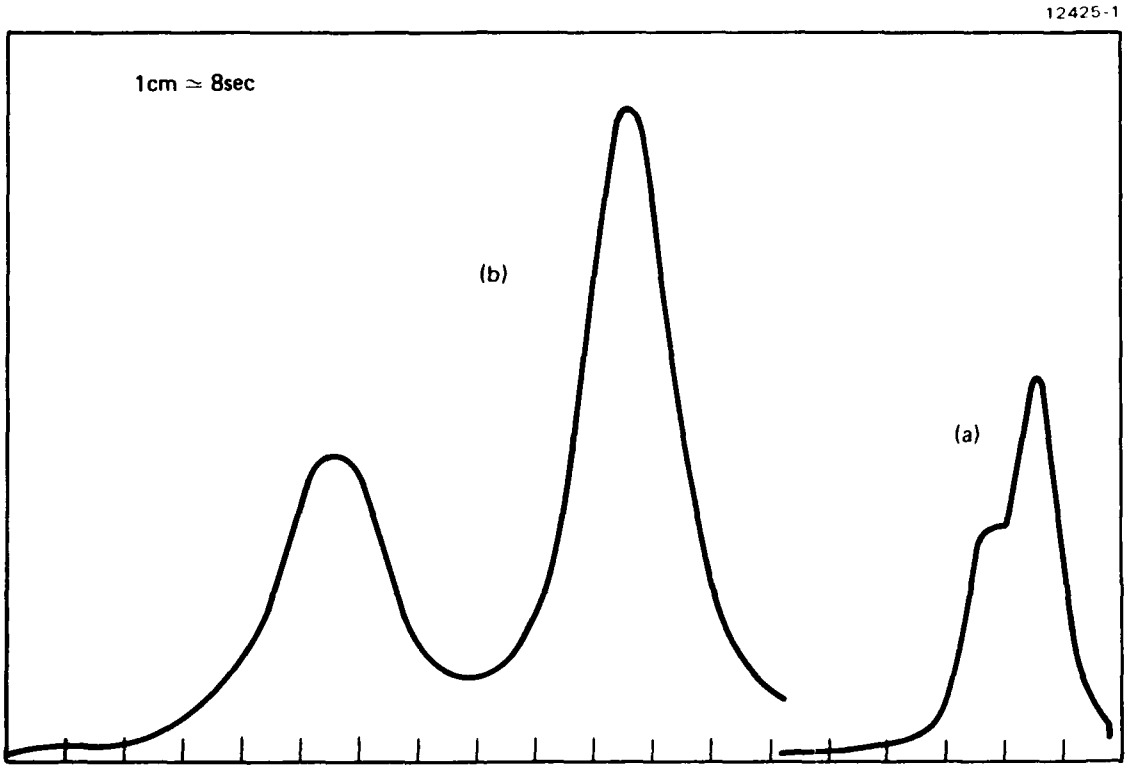

Figure 8. X-ray (rocking curve) data obtained from two InP samples. (a) Chemically polished. (b) Mechanically polished.

SECTION 3

ION IMPLANTATION DOPING STUDIES

A. INTRODUCTION

Ion implantation is a versatile method of doping semiconductors. The dopant concentration and depth of the doped regions can be independently controlled by varying the implantation dose and energy appropriately. The ion implantation process, however, damages the crystal lattice; thus it is necessary to anneal the damage by appropriate heat treatment. This heat treatment supplies the necessary thermal energy to the crystal to ensure that the active dopants are located at the appropriate sites in the lattice and become electrically active.

High temperature annealing of InP is complicated by the excessively high phosphorus vapor pressure over the sample at the anneal temperature. It is, therefore, necessary to encapsulate the sample with an appropriate encapsulant or perform the anneals in a carefully controlled ambient. During the course of these AFOSR-sponsored studies, we have investigated the effectiveness of Sio_2, Si_3N_4, phosphsilicate glass (PSG) and a combination of a thin Si_3N_4 overcoated with PSG as annealing encapsulants. Some of the results from such studies have been reported in earlier reports but will be repeated here for the sake of completeness. We have also annealed some samples in an ambient of flowing phosphilne.

B. ANNEALING STUDIES

Hughes Research Laboratories (HRL) has developed several systems capable of depositing a variety of dielectrics for application to compound semiconductor device processing.

Silicon dioxide and phosphosilicate glass are deposited by a pyrolytic process and silicon nitride by a plasma enhanced deposition process. The results of investigations to evaluate the integrity of these layers following high temperatures annealing are discussed below. SiO_2 films were deposited by a pyrolytic process at 330°C in a cold-wall system operating at atmospheric pressure. The samples were placed on a graphite susceptor which was heated inductively by an rf coil surrounding the reaction chamber. An electronically controlled ramping system ensured that the sample could be brought from 280°C to the deposition temperature (up to a maximum of 750 °C) in a few seconds. Typical gas flow rates used for SiO_2 deposition are:

Nitrogen	42 1/min
SiH_4	11 cm^3/min
Oxygen	210 cm^3/min

The nitrogen flow ensures that the reactor is flushed during deposition and does not enter into the reaction. PSG layers with ~8 atomic percent phosphorus in SiO_2 should be deposited at 330°C by adding 1.9 cm^3/min of PH_3. The PSG films exhibited an index of refraction (EADAX) and Auger Electron Spectroscopy (AES) confirmed that the phosphorus content in these layers are approximately 8%. The silicon nitride layers were deposited by a plasma enhanced deposition process, with the substrates held at ~250°C.

The surface morphology of an InP sample annealed at 700°C for 30 min with SiO_2 encapsulant in the flowing forming gas ambient was examined in a Cambridge 150 stereoscan scanning electron microscope. Examination with the SiO_2 in place revealed the presence of cracks in the encapsulants. On removal

of the SiO_2 layer, shiny tracks on the surface of InP were observed. These are shown in Figure 9. A magnified view of such shiny tracks is presented in Figure 10 and clearly shows extensive surface damage. A X-ray dot map of the same region in Figure 10 from EDAX analysis of the sample is illustrated in Figure 11. The EDAX data is in close agreement to that shown in Figure 15. From this data we conclude that in the regions were the encapsulant ruptured during the high temperature annealing process, a considerble loss of phosphorus ocurred in regions where the molten excess indium solidified (light regions in the micrographs). In the case of samples annealed with phosphosilicate glass (PSG wilth ~8% P in SiO_2) encapsulant, the presence of such surface degradation was considerbly less.

In the case of samples annealed with a thin layer (~400 A) of Si_3N_4 overcoated with ~1000 A PSG layers, little or no surface degradation was observed on annealing at 700°C for 30 min. This anneal process is the base line approach in our InP-based IC program.

We have also annealed InP samples in an ambient of PH_3 and hydrogen. The surface morphology of a sample subjected to such a capless anneal at 730°C for 90 minutes is shown in Figure 12. Little or no surface degradation can be observed. We will investigate the effectiveness of capless annealing in PH_3 ambient as a part of our IR&D program, with a dedicated, properly designed capless annealing furnace.

These studies clearly demonstrate that the use of PSG as an anneal cap is effective in performing the implantation activation annealing process. The results discussed in this section (Figure 12) show that capless annealing in flowing PH_3 ambient is effective in reducing surface degradation. We will evaluate the effectiveness of annealing ion-implanted InP samples in flowing PH_3 ambient in detail with four dedicated capless annealing furnace under an IR&D program.

Figure 9. SEM micrograph of an InP sample annealed with SiO_2 encapsulant at 700°C for 30 min. The shiny regions in this micrograph are In rich regions.

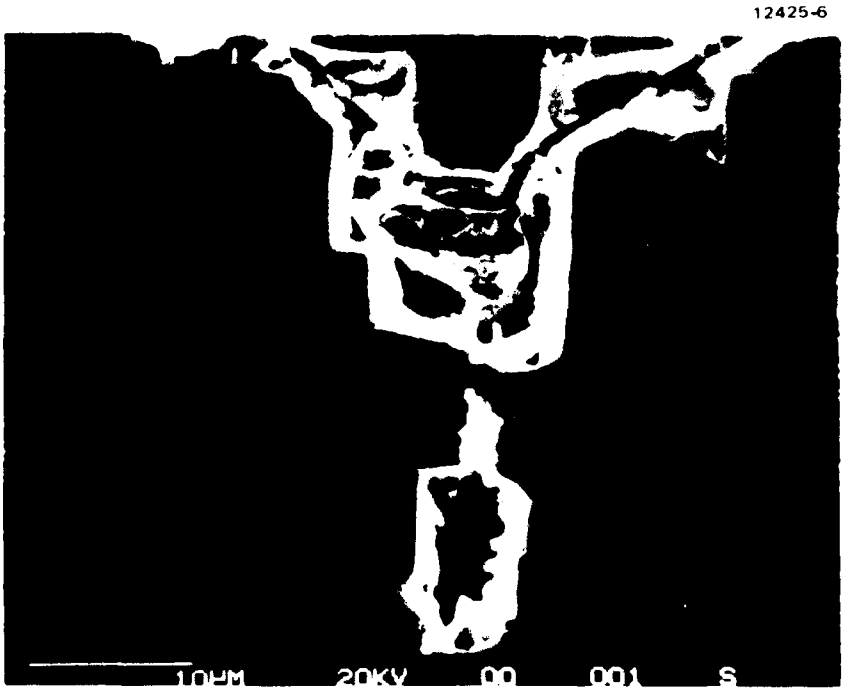

Figure 10. A magnified view of an In rich region from the sample shown in Figure 9.

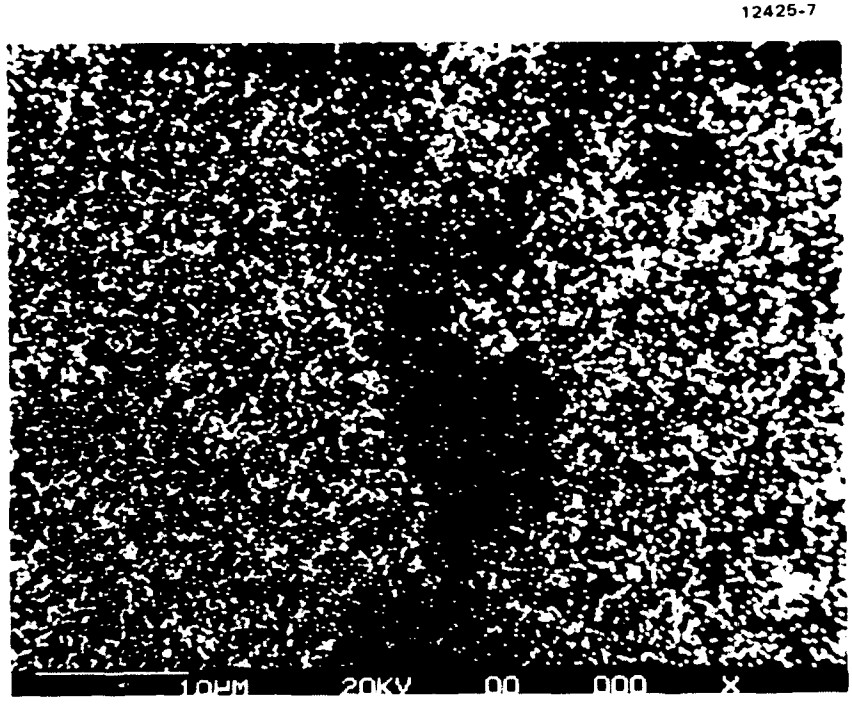

Figure 11. X-ray dot elemental image of region in Figure 10. The figure shows the distribution of indium.

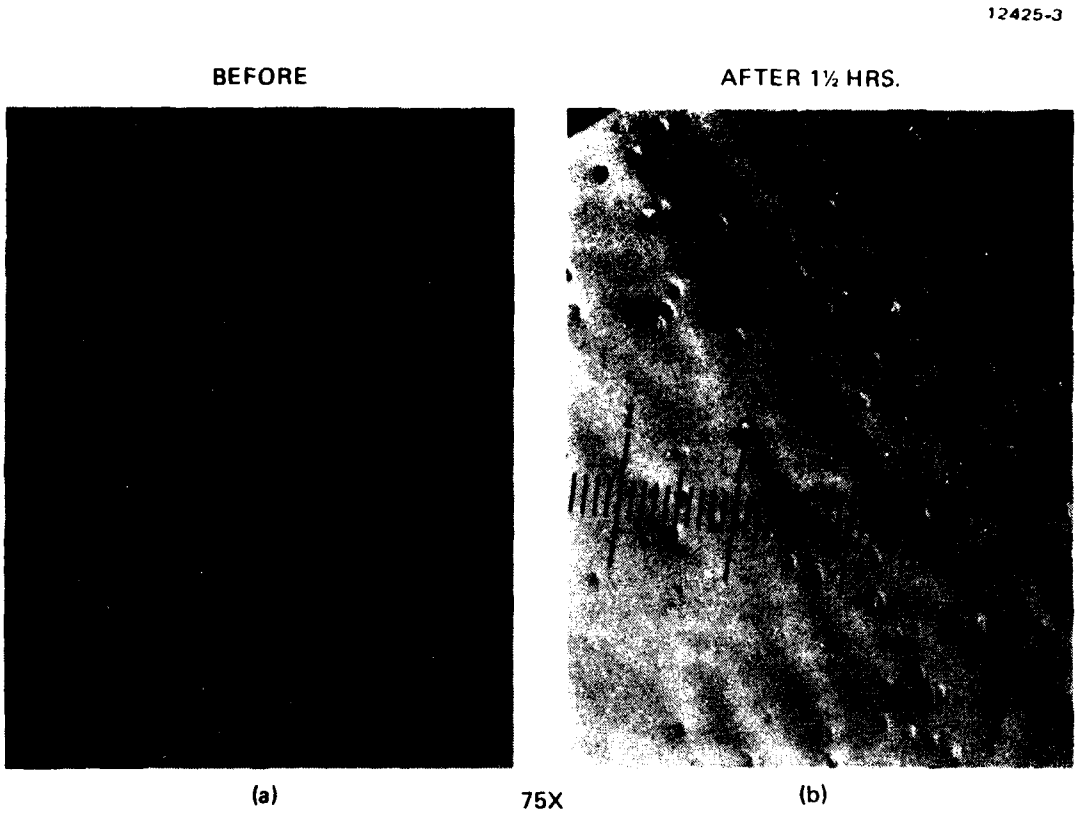

Figure 12. Decomposition of InP substrate at 730°C in H_2 ambient with PH_3.

C. ELECTRICAL EVALUATION OF ION IMPLANTED LAYERS

Hall effect measurements were performed on ion implanted and annealed InP samples. The process parameter studied included various dopant ions, implant temperature, energy, fluence, anneal temperature and the use of different encapsulants during anneal. Both p-type (Be) and n-type dopants (C, Si, Si, Sn, and Se) were studied. The details of such studies are described in this section. The results show that it is easier to achieve high donor doping levels. Secondary ion mass spectrtometry (SIMS) studies show that little or no redistribution effects occur following high temperature annealing with n-type dopants, even at high concentrations. In contrast dramatic redistribution can be seen in high dose Be-implanted samples. They become evident even at anneal temperatures as low as ~650°C.

Preliminary SIMS studies show the redistribution of Fe in ion-implanted and annealed InP samples. The redistribution of Fe in implanted InP is qualitatively similar to the redistribution of chromium in horizontal Bridgeman-grown semi-insulating GaAs. However, quantitative determination of the extent of Fe redistribution require extensive measurements.

1. Be-Implanted InP

Beryllium is known to be a shallow acceptor in several III-V compound semiconductors. It has an atomic mass of 9 and causes little damage to the lattice. Extensive optical studies in GaAs have shown that the lattice damage introduced by Be anneal out at ~400°C, and that almost complete electrical activation can be accomplished at an anneal temperature as low as 500°C.

The measured sheet hole concentration and the hole mobility are plotted in Figure 13 as a function of anneal temperature from InP samples implanted with 300 keV Be^+ to the fluences indicated. At low doses, the measured sheet hole concentration increases monotonically with anneal temperature. Over 80% of the implanted Be becomes electronically active following an anneal at 750°C for 30 min. In the case of high dose (1×10^{14} cm^{-2}) implanted samples, the maximum percentage activation (~65%) was measured in samples annealed at ~700°C. The measured sheet carrier concentration decreased slightly on annealing at 750°C. There was a slight but gradual increase in hole mobility with increased anneal temperatuare.

In order to establish a threshold anneal temperature for electrically activating Be in InP, samples were implanted with 100 keV Be to fluences ranging from 1×10^{13} cm^{-2} to 1×10^{14} cm^{-2}. All the samples were encapsulated at 330°C with phosphosilicate glass and were subjected to higher temperature anneals for 30 min in an ambient of flowing, forming gas. The lowest anneal temperature used in this study was 330°C (same as PSG deposition temperature). Following the anneal and removal of PSG, ohmic contacts were formed and the samples were electrically evaluated. Figure 14 shows the variation of measured carrier concentration as a function of anneal temperature for the Be-implanted samples. For anneal temperatures between 330°C and 400°C, the samples remained high resistivity n-typle (carrier concentrations ~10^8 el/cm^2). It appears that implantation-induced defects in InP are donor-like centers. However, at anneal temperatures between 500°C and 550°C the layers become strongly p-type, with a large fraction of the implanted dopants becoming electrically active. This sharp annealing threshold is similar to the annealing behavior of Be-implanted GaAS.

We have used SIMS to obtain the atomic distribution of Be from as-implanted and annealed samples. Figure 15 shows the as-implanted distribution of Be-implanted to a dose of 3×10^{13} cm^{-2}

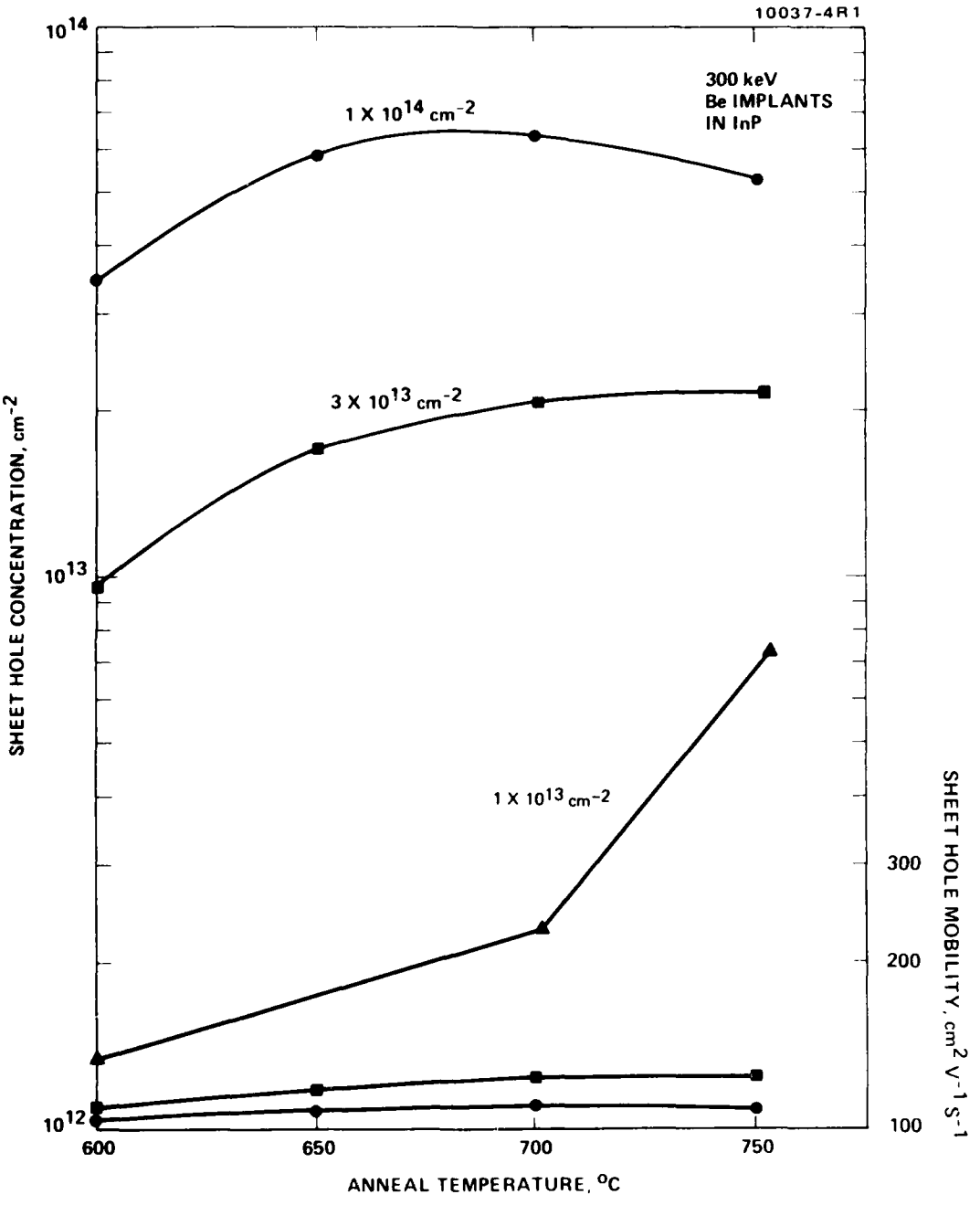

Figure 13. Measured sheet hole concentration and hole mobility as a function of anneal temperature from InP samples implanted with beryllium to fluences shown.

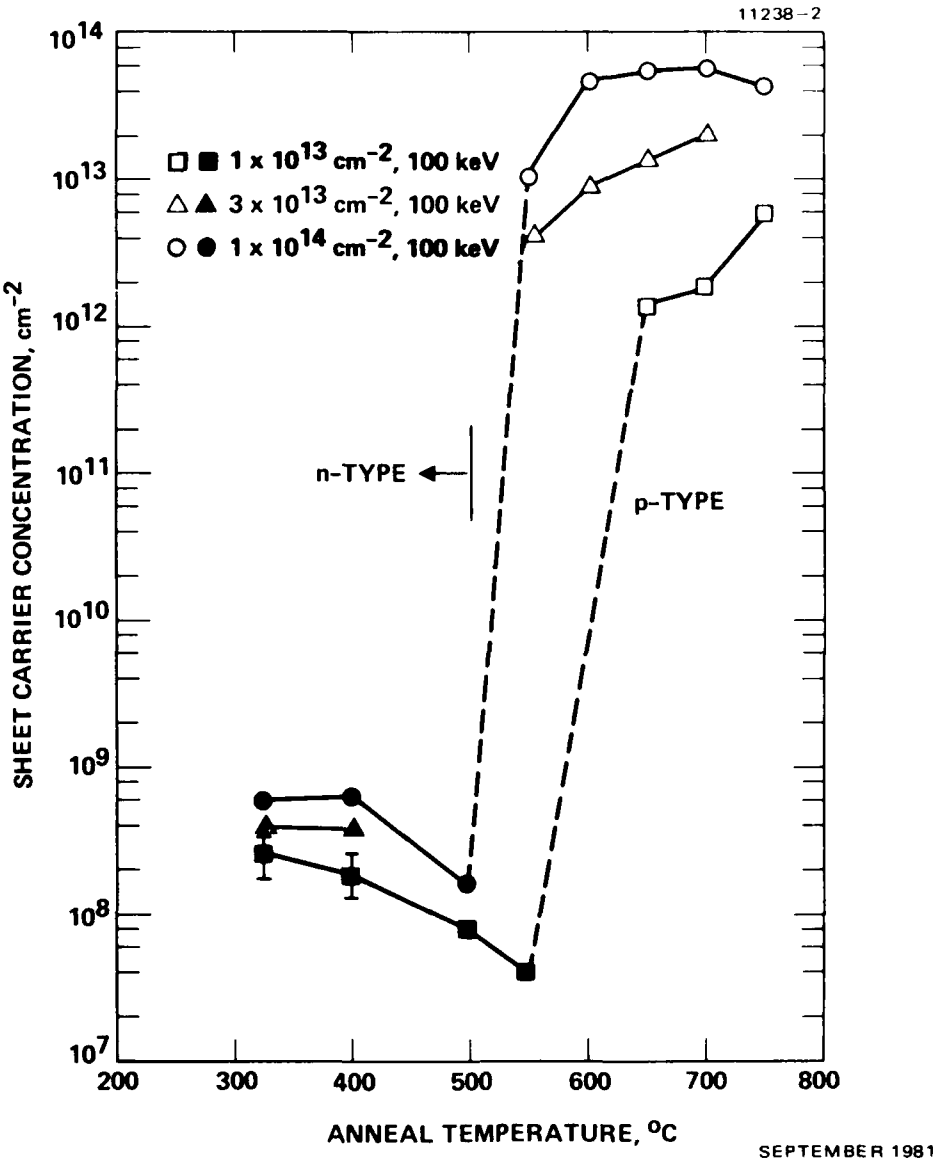

Figure 14. Measured sheet carrier concentration as a function of anneal temperature from Be-implanted InP samples.

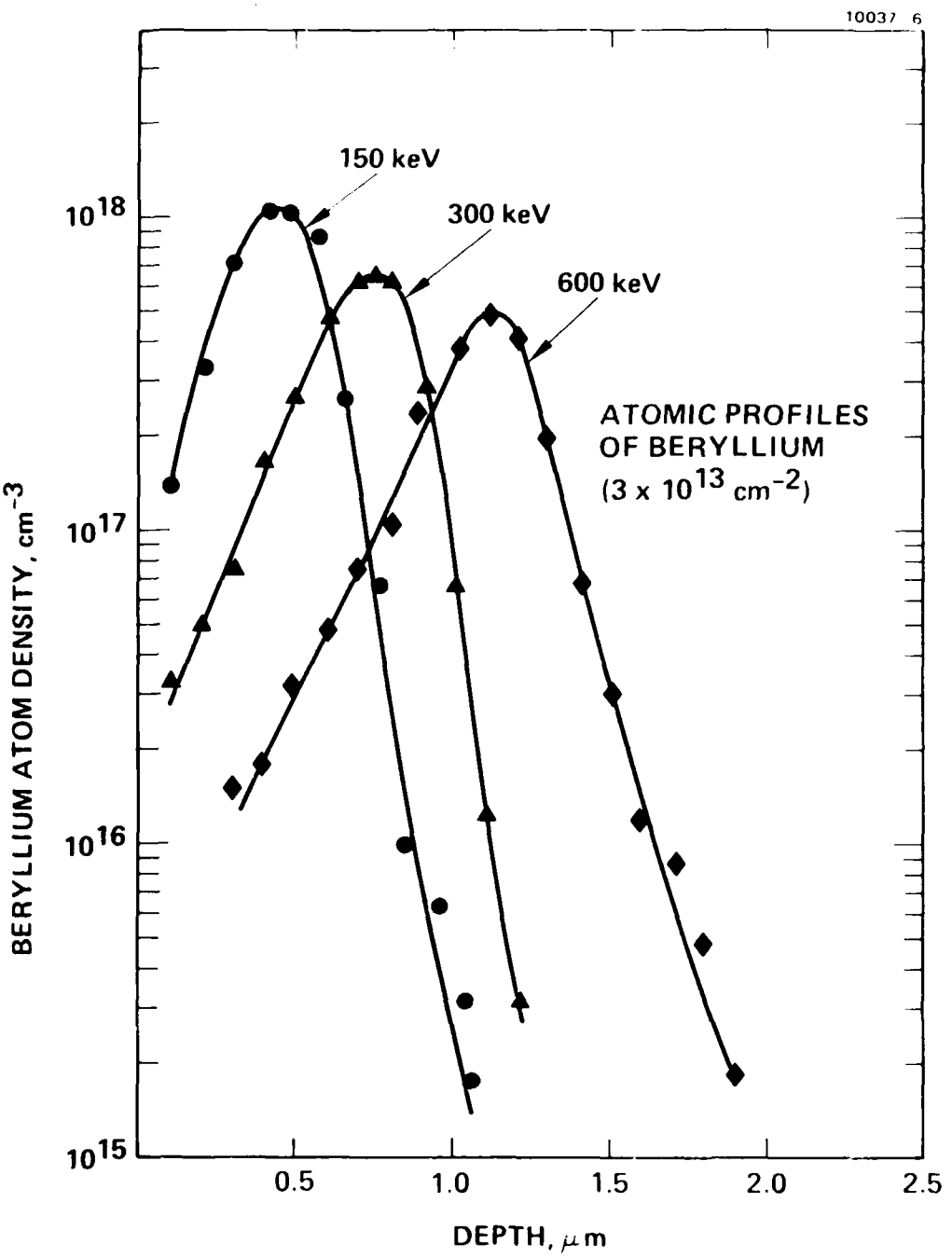

Figure 15. Atomic distribution of ion-implanted Be in InP. The implant energies were 150 keV, 300 keV and 600 keV with an implant fluence of 3 x 10^{13} cm-2.

at energies of 150 keV, 300 keV, and 600 keV. The depth scale (x-axis) was calibrated by measuring the depth of the SIMS craters with a Sloan Dektak system. The atomic concentration (y-axis) can be calibrated by assuming that the integrtaed be atom concentration within the Gaussian is equal to the implant fluence. The peak of the distribution occurs at nearly the projected range, as calculated by LSS theory. The shape of the dopant profile is not symmetrical and appears to be skewed to the surface. With a light projectile like Be thrust in a target composed of heavy elements like InP, such skewing towards the surface is expected. Such non-symmetrical profiles can be described by a modified Pearson IV distribution.

In the case of low fluence implants (1×10^{14} cm^{-2}, 300 keV) annealed (700°C, 30 min with PSG encapsulant) Be profiles do not differ significantly from the as-implanted profile. In the case of samples implanted to a fluence of 1×10^{14} cm^{-2}, dramatic redistribution effects can be observed, even in samples annealed at 650°C for 30 min. The as-implanted and annealed (650°C and 700°C anneals) Be profiles obtained from InP samples are shown in Figure 16. The results are qualitatively similar to the annealing behavior of high fluence Be-implanted GaAs, except that some features in the redistributed profiles are different. A more detailed and thorough study of such redistribution effects needs to be performed to understand this effect.

2. Electrical Evaluation of n-Type Dopants

Among all potential n-type dopants in InP, carbon has the lightest atomic mass. It is only slightly more massive than Be, and the damage introduced by C is not expected to be very different from that due to Be. Since Be can be activated at an anneal temperature as low as 550°C (as shown in the previous section), we decided to investigate the annealing behavior of carbon-implanted InP.

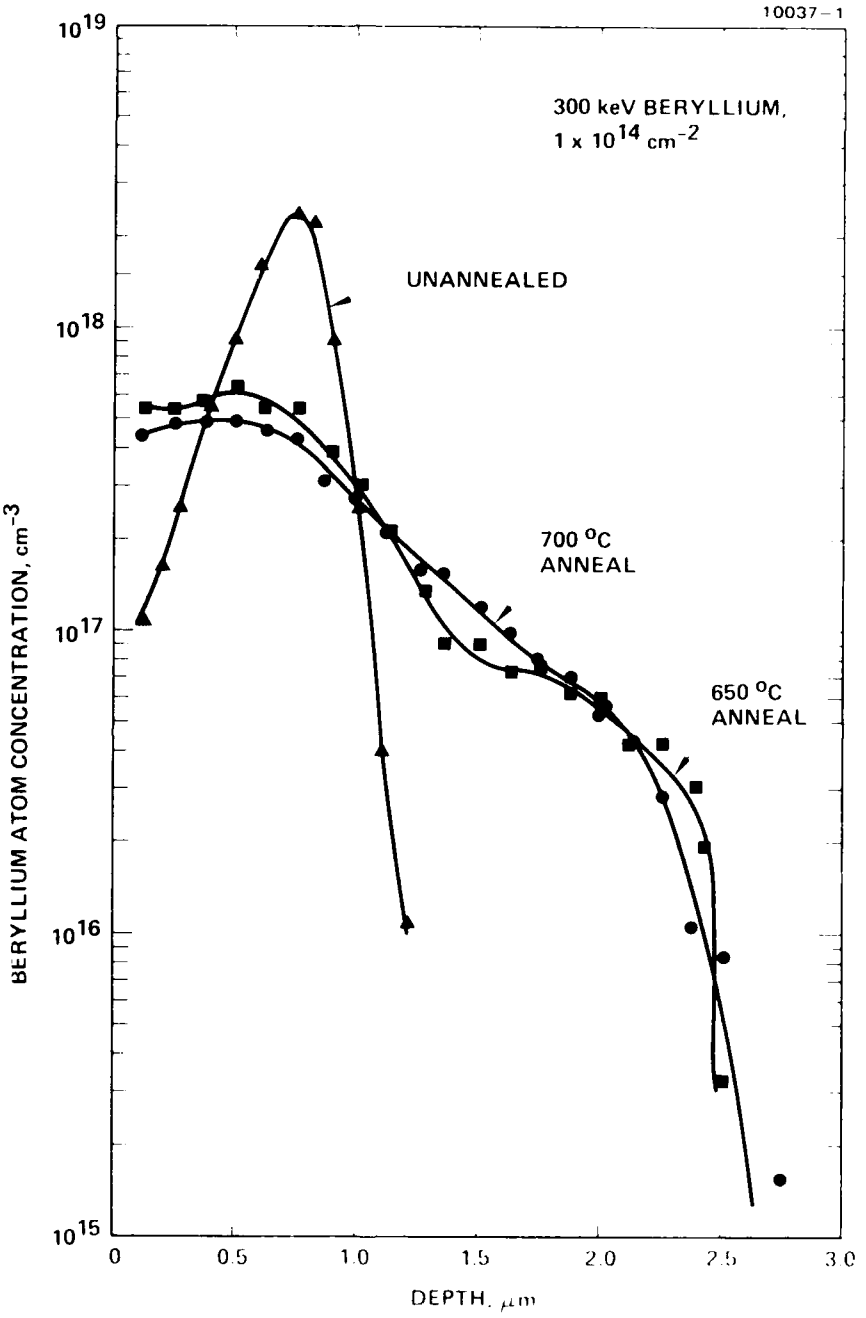

Figure 16. Atomic distribution of ion-implanted Be obtained from unannealed and annealed InP samples showing effects of drastic redistribution.

Samples were implanted with 200 keV C^+ to doses ranging from 1 x 10^{13} cm^{-2} of 2 x 10^{14} cm^{-2}. These samples were encapsulated with PSG and annealed at temperatuares ranging from 550°C to 750°C. Electrical measurements show that only ~3% of the implanted dopants became donor-like, even after annealing at 700°C. Annealing at 750°C for 30 min, did not increase percentage activation substantially. Electron mobilities measured in 750°C annealed, low fluence (1 x 10^{13} cm^{-2}), implanted samples were only 2000 cm^2 $V^{-1}s^{-1}$. The low electrical activation and low measured carrier mobilities encountered in C^+ implanted InP leads us to spectulate that carbon acts as an amphoteric dopant in InP. Low temeprature photoluminescence and local mode vibrational spectroscopic measurements and annealed InP samples may provide some answers. Another explanation may be that most of the carbon atoms on annealing occupy interstitial sites. Regardless of the mechanism involved, carbon does not appear to be efficient n-type dopant in InP.

Silicon, which is a group IV element, is a potential n-type dopant in InP. Although silicon is an amphoteric dopant in III-V semiconductors, silicon introduced by ion implantation acts primarily as a donor in GaAs. The present studies clearly show that a similar trend holds good in InP and that silicon is a well-behaved donor dopant in InP.

A wide range of implantation and anneal parameters were convered in this study, including implant doses from 3 x 10^{12} cm^{-2} to 1 x 10^{14} cm^{-2}, which an implant energy of 300 keV. Some implants were also performed at 100 and 600 keV. These samples were annealed over a temperature range from 650°C to 750°C. Most of the studies described in this seciton were performed using PSG as the annealing encapsulant. Results obtained from samples annealed with a thin Si_3N_4 (~400 Å) and overcoated with PSG were essentially indistinguishable from samples annealed with a SPG encapsulant along.

As seen in Figure 17, in the case of flow fluence implanted samples ($<3 \times 10^{12}$ cm^{-2}), over 80% of implanted atoms became electrically active on annealing at ~750°C for 30 min. Carrier mobilities as high as 2900 cm^2 $V^{-1}s^{-1}$ were measured in 5×10^{12} cm^{-2} implanted samples annealed at 750°C. In the case of high fluence implanted samples ($>6 \times 10^{13}$ cm^{-2}), the measured sheet electron concentration appeared to saturate at ~5×10^{13} cm^{-2} following an anneal at 750°C for 30 min. At such concentrations, typical mobilities of 1500 cm^2 $V^{-1}s^{-1}$ were measured.

It is more informative to plot the measured carrier concentration as a function of implantation fluence for various anneal temperatures. Such information is summarized in Figure 18. The complete (or 100%) activation line is shown by the dotted line in this figure. The three solid curves represent the data obtained from samples which were annealed at 650, 700, and 750°C, respectively. As seen from this figure, it is clear that for samples implanted to fluences ranging from 8×10^{12} to 4×10^{13} cm^{-2}, over 90% electrical activation can be achieved following an anneal at 750°C. The data shown for silicon represents the average data from a large number of InP samples and represents the baseline implant process for forming the source-drain regions for our MISFET IC program.

We have also evaluated the as-implanted and annealed (700°C, 30 min with PSG encapsulant) profiles of silicon-implanted at InP. The data, shown in Figure 19, show little or no difference between the as-implanted and annealed profiles, even at high silicon atom concentrations. This data clearly indicates that in contrast to the behavior of Be (acceptor)-implanted InP, silicon implanted InP exhibits little or no redistribution behavior in InP even at concentrations in excess of 1×10^{18} cm^{-3}.

Germanium is another amphoteric dopant in III-V compound semiconductors. Depending upon the implantation (implant fluence and temperature) and process parameters (annealing temeprature, encapsulant used) implanted Ge can either act as

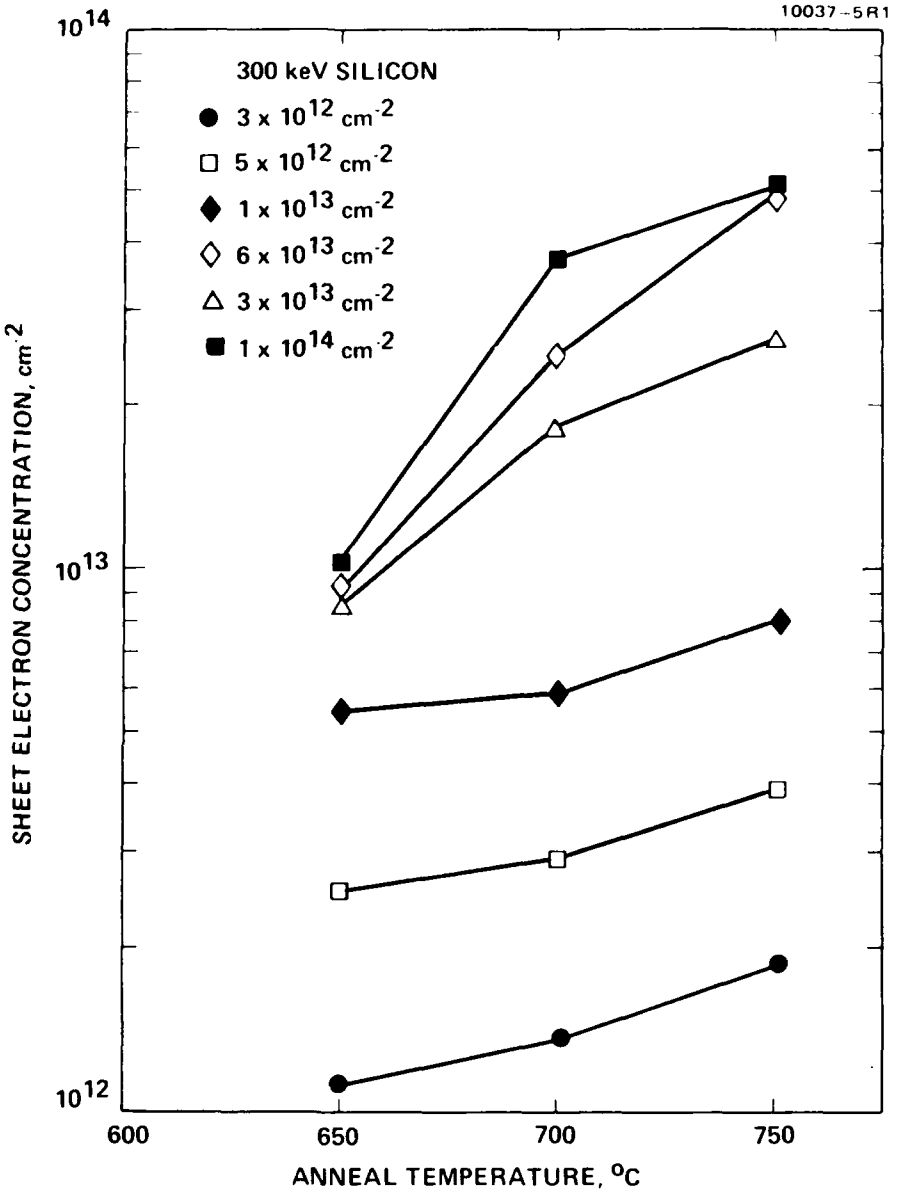

Figure 17. Sheet electron concentration as a function of anneal temperature in InP samples implanted with silicon ions to fluences indicated.

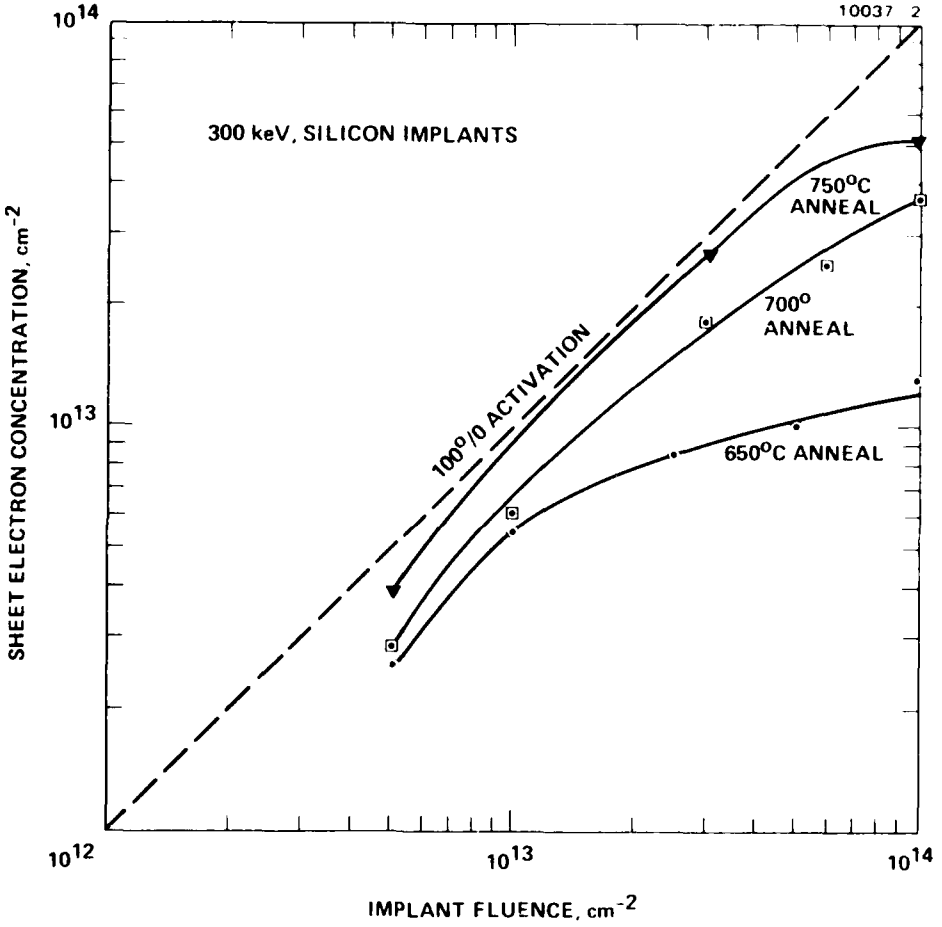

Figure 18. Sheet electron concentration as a function of implant fluence of 300 keV Si-implanted InP samples.

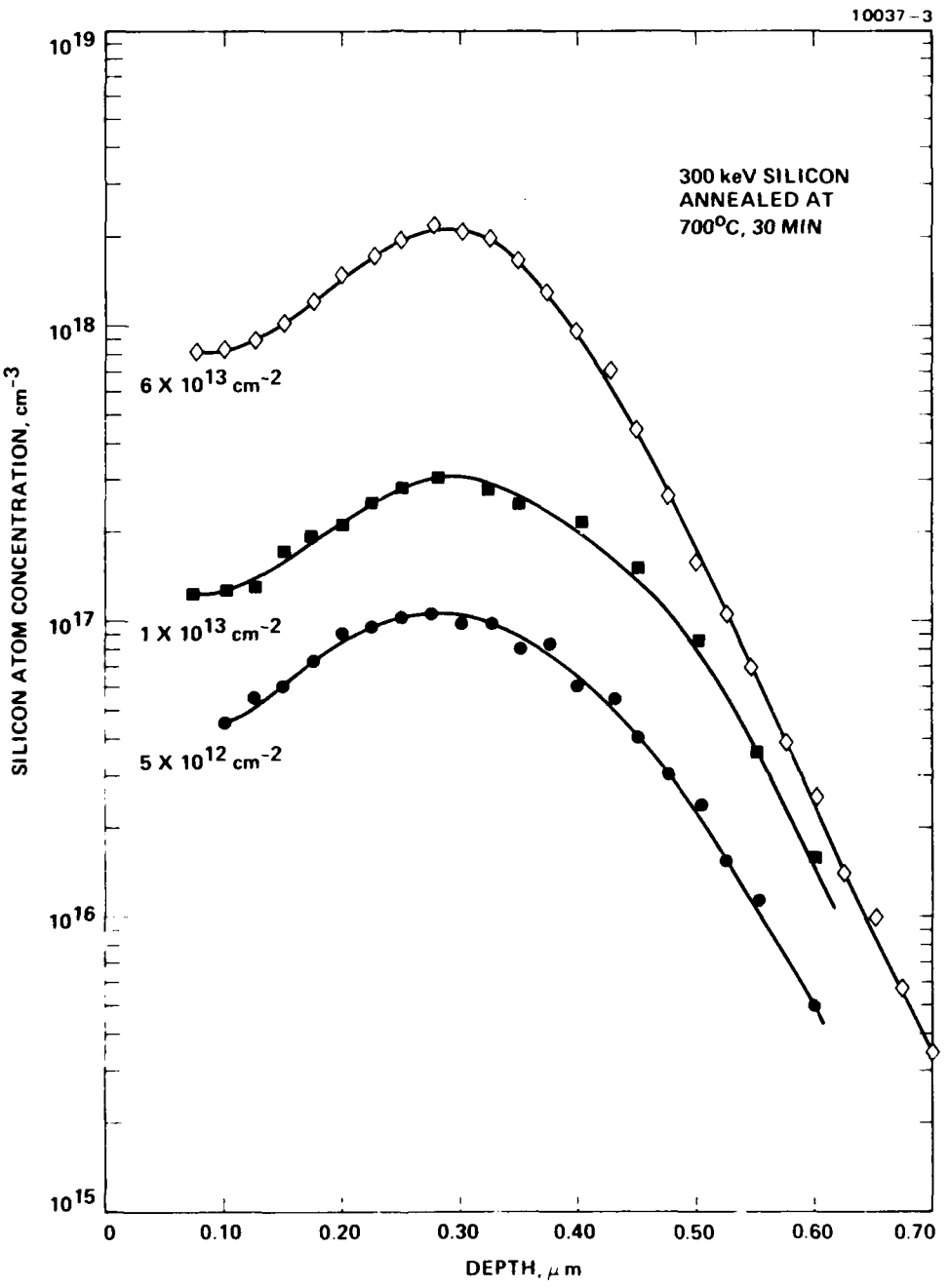

Figure 19. Atomic distribution obtained from Si implanted and annealed InP samples.

a donor or as an acceptor in GaAs. We have investigated the annealing behavior of InP samples implanted with Ge. For the conditions covered in this study, all Ge-doped layers exhibited strong n-type conductivity with a high degree of carrier activation.

Several InP samples were implanted with Ge to fluence ranging from 6 x 10^{12} cm^{-2} to 3 x 10^{11} cm^{-2}, with implant energies of either 150 keV, 300 keV, or 600 keV. The samples were encapsulated with either PSG or Si_3N_4 and were annealed at temperatures ranging from 650°C to 750°C for 30 min.

The variation of mesured sheet electron concentration and sheet electron mobility are shown as an implant fluence in Figure 20 for anneal temperatures of 650, 700, and 750°C. All these data were obrtained from samples implanted with 600-keV Ge ions. The complete (100%) activation curve is also shown (by the dashed line) in this figure. For the intermediate dose range (from 6 x 10^{12} cm^{-2} to 5 x 10^{13} cm^{-2}), high carrier activation is achieved on annealing at 750°C. For much higher doses, the activation efficiency decreases to ~40%. The measured mobilities in 750°C -annealed samples range from ~2200 cm^{-2} $V^{-1}s^{-1}$ (low fluence) to ~650 cm^2 $V^{-1}s^{-1}$ (high fluence). We also observed that higher activation with high carrier mobilities were achieved in samples with higher energy ions. For example, in samples implanted with 600 keV, 3 x 10^{13} cm^{-2} Ge ions and annealed at 750°C sheet carrier concentrations of 2.3 x 10^{13} cm^{-2} and mobilities of 1280 cm^2 $V^{-1}s^{-1}$ were mesured while the same fluence at 150 keV and annealed at 750°C exhibited sheet carrier concentrations of 1.9 x 10^{13} cm^{-2} with cm^{-2}, with carrier mobilities of 730 cm^2 $V^{-1}s^{-1}$. These data indicate that the residual defects in the near surface region play a major role in carrier transport properties of Ge-implanted InP. Preliminary data indicates that high fluence of implants at 150°C show higher carrier activation and higher carrier mobilities than

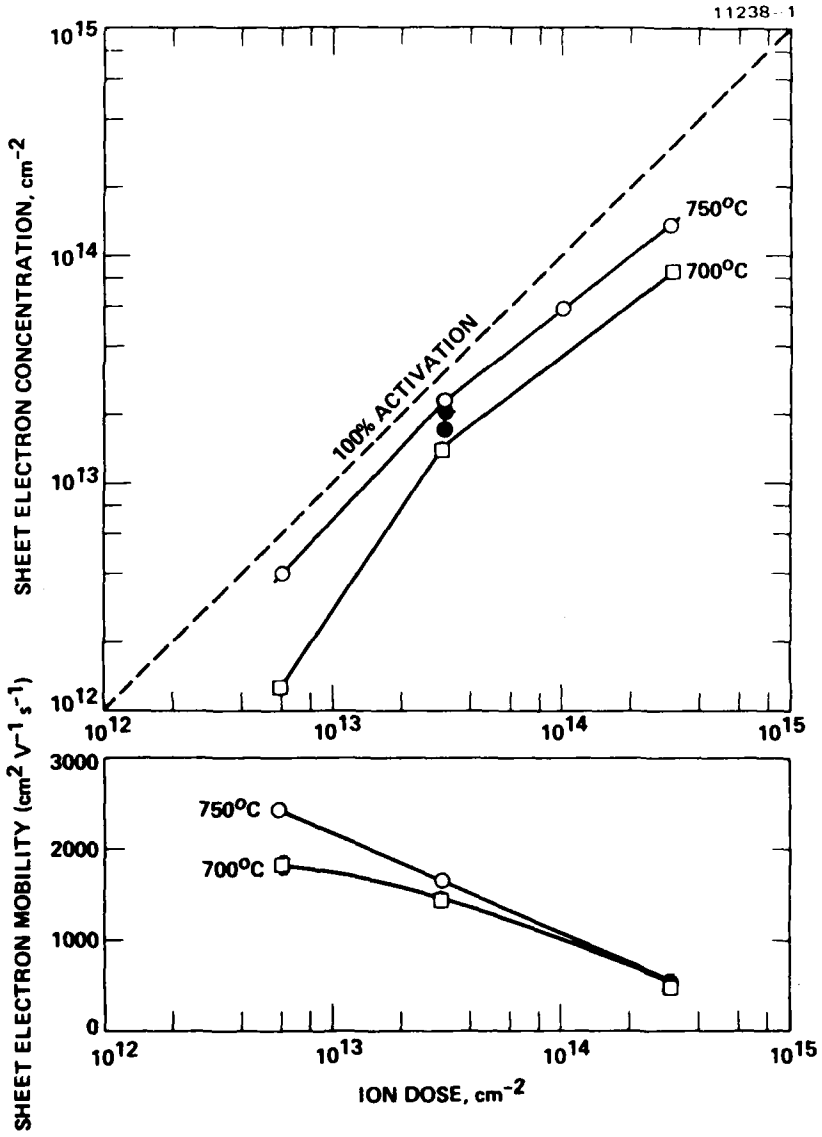

Figure 20. Sheet electron concentration and sheet electron mobility in Ge-implanted InP samples as a function of implantation dose and annealed at 700°C and 750°C.

room temperature implants. Also samples annealed with PSG encapsulation exhibit higher degree of electrical activation.

The distribution of Ge atoms, as obtained by SIMS measurements, from as-implanted and annealed (750°C) InP samples are shown in Figure 21. The experimental data show that little or no redistribution of implanted Ge takes place on annealing, even at high concentrations. These results are in agreement with data from Si-implanted samples, but are in complete contrast to the atomic redistribution observed in Be-implanted and annealed samples. Drastic diffusional broadening of other acceptor-implanted dopants (Zn, Cd, Mg) are known to occur in InP and other III-V compound semiconductors.

Preliminary experiments on Sn-doped InP layers indicate that Sn is a well-behavied donor dopant in InP. Table 3 describes the results obtained form 150 keV, 300 keV, or 600 keV Sn^+ implants (3×10^{13} cm^{-2}). The data clearly demonstrate that high activation can be achieved in samples implanted with

Table 3. Electrical Properties of Sn-Implanted InP
Implant Fluence: 3×10^{13} cm^{-2}

Energy, keV	Anneal Temperature, °C	Sheet Electron Concentration, cm^{-2}	Sheet Electron Mobility, $cm^2\ V^{-1}s^{-1}$
150	700	$(1.08 \pm 0.05) \times 10^{13}$	1200 ± 10
300		$(1.72 \pm 0.05) \times 10^{13}$	1310 ± 40
600		1.73×10^{13}	1531 ± 52
150	725	$(1.86 \pm 0.15) \times 10^{13}$	1330 ± 70
300		$(2.08 \pm 0.04) \times 10^{13}$	1429 ± 80
600		$(2.06 \pm 0.02) \times 10^{13}$	1698 ± 72

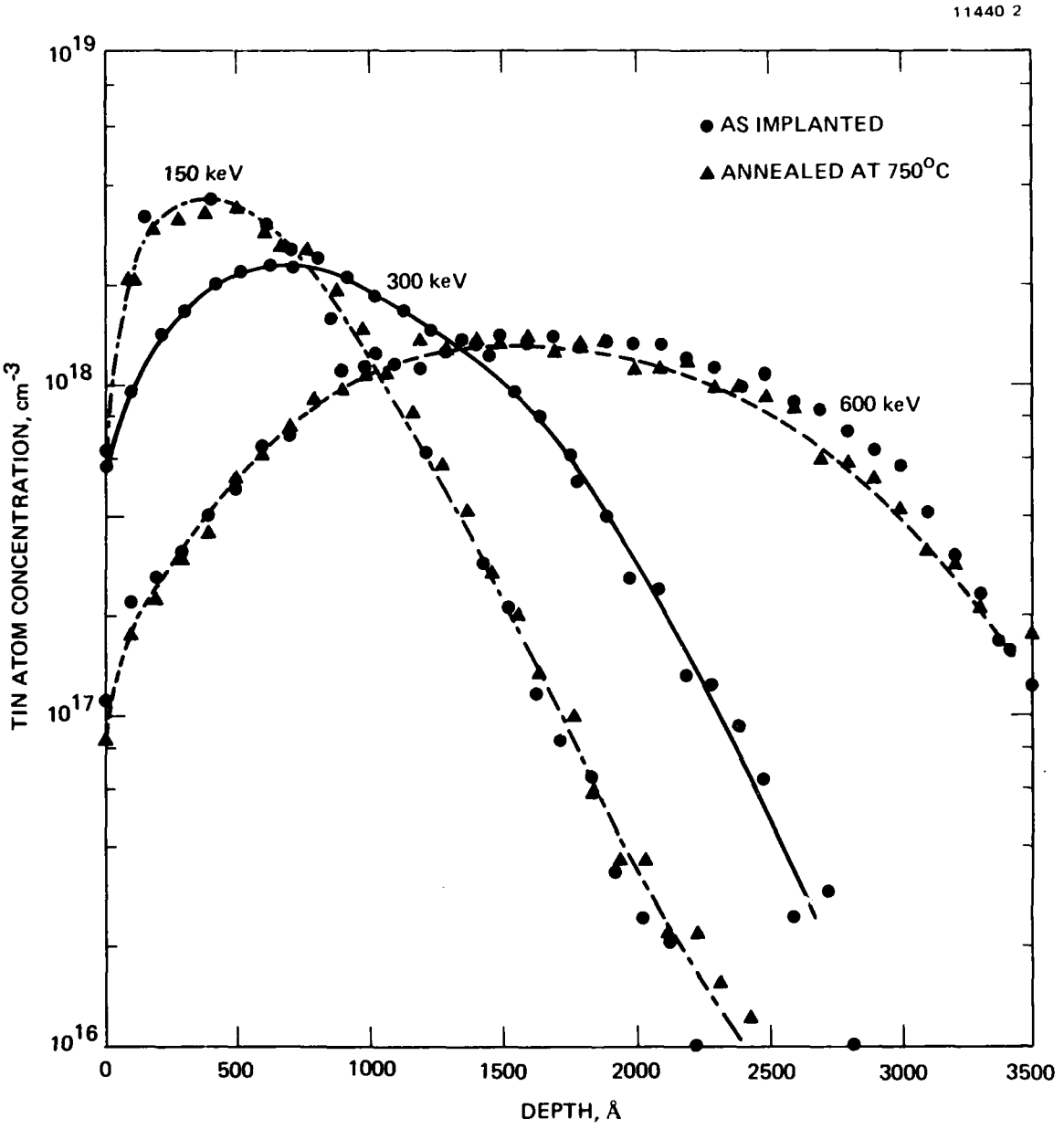

Figure 21. SIMS atomic distributions of Ge obtained from As-implanted and annealed InP samples.

Sn at elevated temperatures. These experimental results show that recrystallization of heavily damaged or amorphorized compound semiconductors is a major problem. The mechanisms involved in recrystallization of amorthized compound semiconductors are not well understood. Some preliminary time resolved reflectivity (TRR) measurements indicate that random nucleation process may be a dominant process in recrystal-lizaiton and amorphized compound semiconductors.

In Figure 22 we show the SIMS atomic distribution of Sn in implanted and annealed InP. Three differtent implant energies were used and the anneals were performed at 725°C for 30 minutes with PSG encapsulation. The annealed atomic distribution does not differ significantly from the as-implanted distribution. These results show that none of the n-type dopants studied in this program diffuse significantly during the activation anneal. This is distinctly difference from the behavior of p-type dopants, most nobility that of Be.

We have also investigated the annealing behavior of Se-implanted InP. In Figure 23, we show the variation of measured sheet electron concentration and sheet mobility as a function of implantation dose for two implant temperatures. As seen from this data the anneal behavior of Se in InP is the same as those of Si, Ge, and Sn-implanted samples. For all fluences converted in this study, Se implants performed at ~150°C show a higher degree of electrical activation. The 150°C implanted samples show higher electron mobilities compared to room temperature implanted samples.

D. REDISTRIBUTION OF Fe IN ION IMPLANTED AND ANNEALED InP

The thermal stability of semi-insulating InP following high temperature processing is closely related to the redistribution of the deep level dopant (in this case, Fe) during such thermal treatment. As discussed in an earlier section, there is a problem in quantitative determination of the concentration of Fe

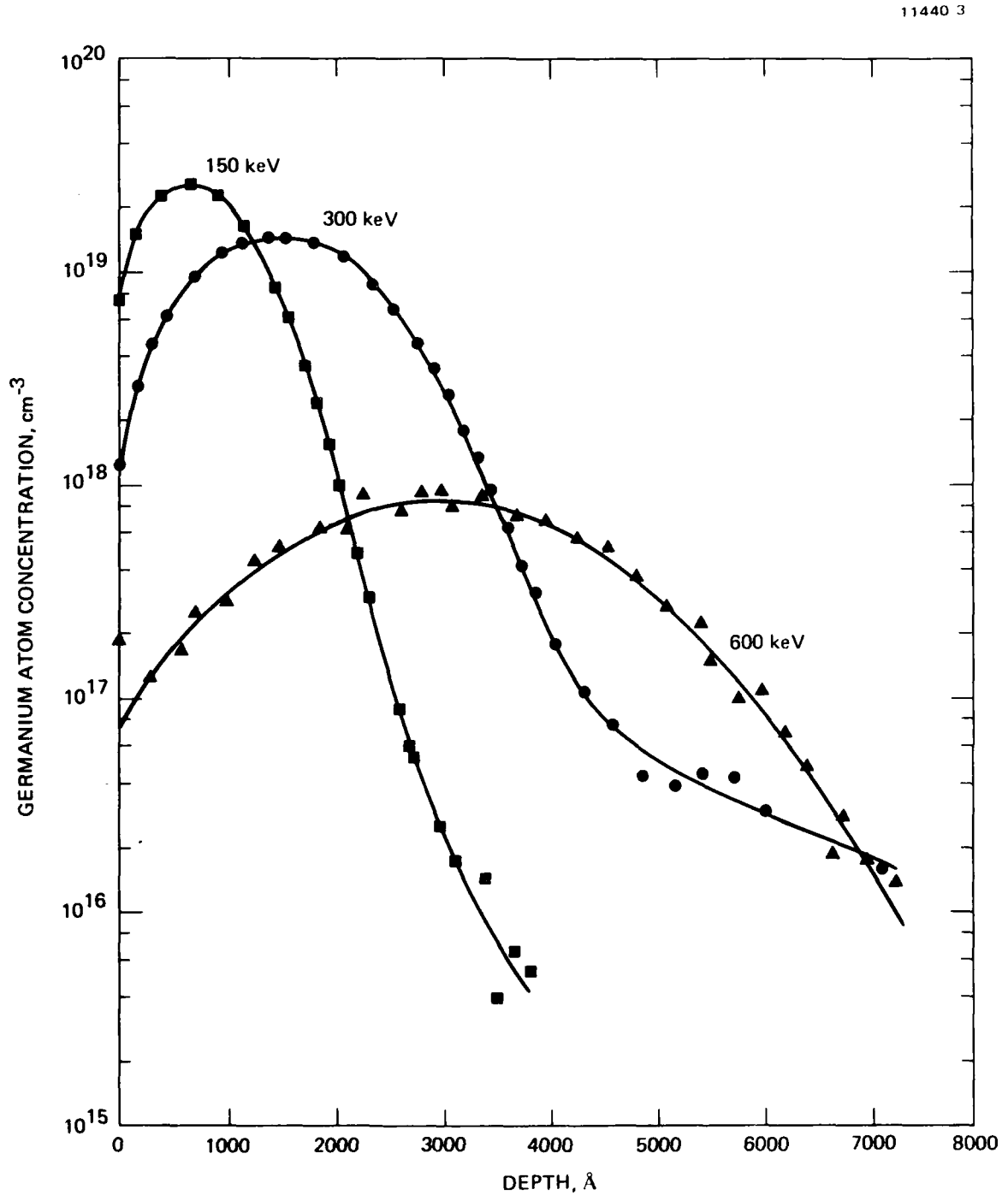

Figure 22. SIMS atomic distribution obtained from Sn-implanted and annealed InP.

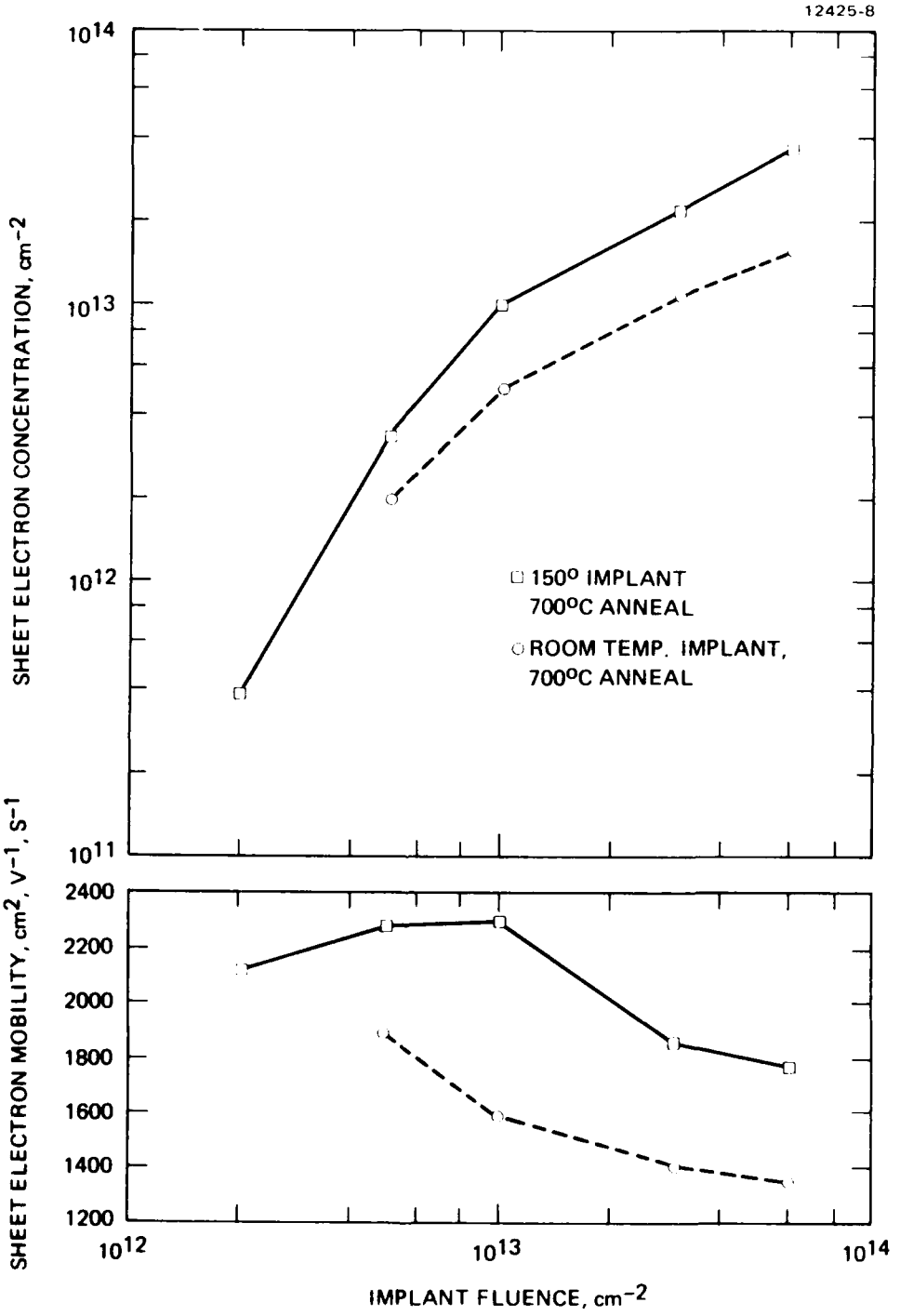

Figure 23. Electrical properties of Se-implanted InP.

by SIMS. Useful qualitative depth distribution can, however, be obtained using this technique.

We have performed a series of experiments to determine redistribution effects of Fe in Sn-and Ge-implanted and annealed InP. These data are presented in Figures 18 and 19. For example,. the data from samples implanted with 300 keV and 600 keV sn-implanted samples (3×10^{13} cm^{-2}) and annealed at 700°C and 750°C are shown in Figures 24 and 25 respectively. Inspection of these figures clearly reveals that in all cases dramatic Fe-redistribution effects are observed. There is a pile up of iron at the surface, followed by a depletion at the point of maximum damage (at a depth shallower than the projected range), followed by a gradual recovery to bulk doping levels. The effects observed are similar to the reported redistribution effects of chromium in GaAs. While there are questions about the quantitative determination of Fe in InP by SIMS analysis, we believe the observed redistribution of Fe is qualitatively correct. The data presented here is too preliminary to be useful for evaluating the diffusion coefficient of Fe in InP.

We have also studied the depth distribution of Fe in InP samples encapsulated with PSG or Si_3N_4 and annealed at 725°C for 30 minutes. These samples did not receive any implants. No drastic redistribution of Fe, as seen in implanted and annealed samples (Figures 24 dand 25), was observed. This leads us to believe that the redistribution of Fe is aided by the presence of large concentrations of defects in the implanted region. More experiments need to be performed to understand this phenomenon.

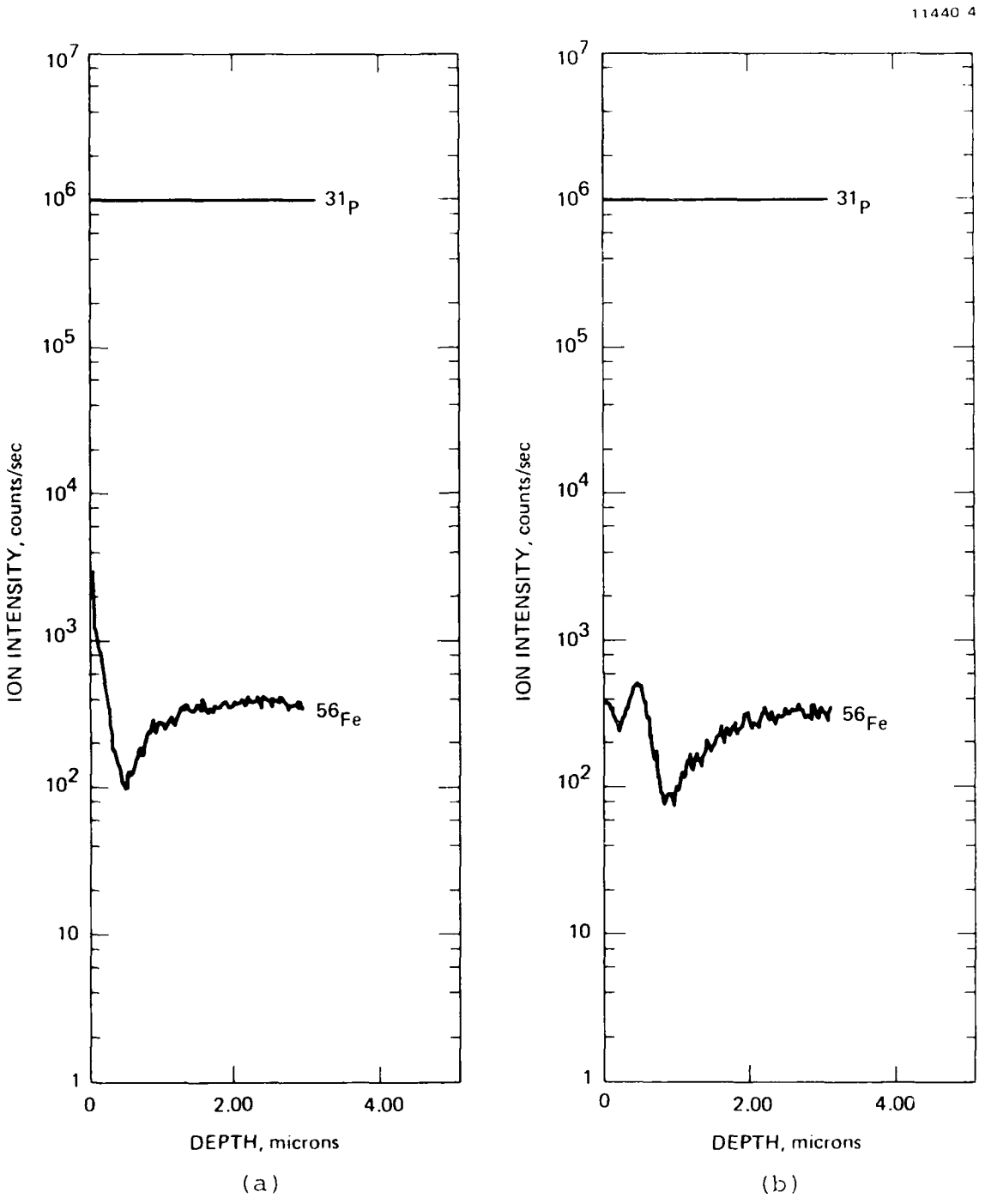

Figure 24. Atomic distribution of iron in Sn-implanted InP samples annealed at 700°C for 30 min.
(a) 300 keV implant (b) 600 keV implant

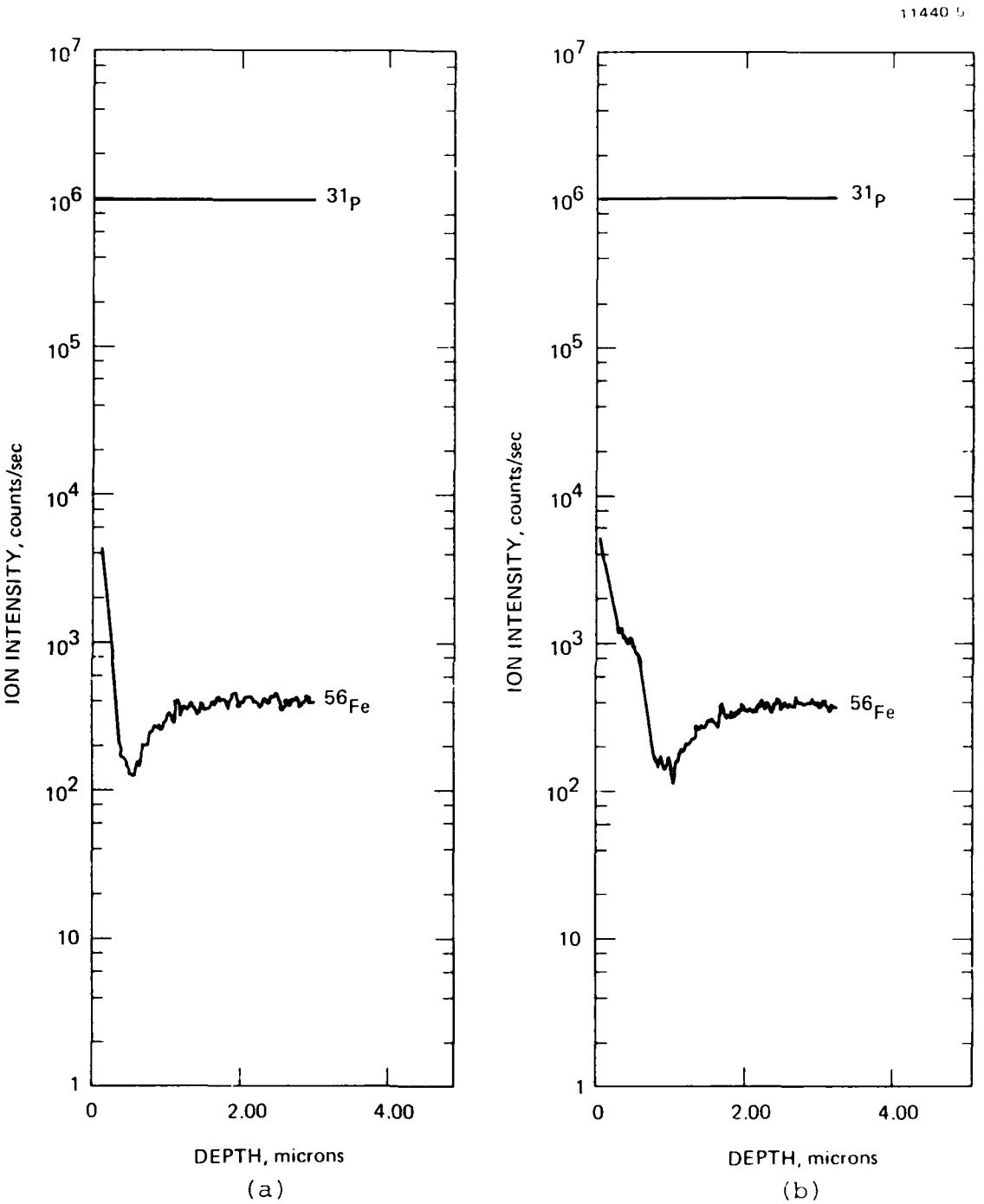

Figure 25. Atomic distribution of iron in Sn-implanted InP samples annealed at 750°C for 30 min.

(a) 300 keV implant (b) 600 keV implant

E. RUTHERFORD BACKSCATTERING STUDIES

The backscattering studies were performed by using a system developed at HRL. The system is capable of operating at 150 kev. H^+, He^+, and He^{++} ions can be used to perform the RBS analysis. The use of He^{++} permits the experiments to be performed at 300 keV. The ion optics in the system provide a well-collimated beam with beam divergence of less than 0.1°. The target to be analyzed is mounted on a goniometer. By using this goniometer, we can align the sample with respect to the beam to within 0.02°. The analysis is performed by detecting the backscattered particles with a cooled surface barrier detector. A Canberra model 8-0 multichannel analyzer, in conjunction with a DEC PDP-11 computer system, is used to analyze the pulses obtained from the detector and results in the display of the number of backscattered particles as a function of energy.

The analysis of the data allows us to determine the degree of crystallinity or damage formation, the depth of the damaged layer (provided it is not much deeper than 2,000 Å from the surface) and the location of dopants in the lattice by performing channel measurements, provided the dopant atoms are more massive than the substrate atoms.

A sample of InP was implanted with Si^+ at 100 kev. By using appropriate metal masks, different portions of the sample were implanted to fluences ranging from 2×10^{12} cm^{-2} to 6×10^{13} cm^{-2}. The RBS spectra obtained from these regions as well as from a non-implanted region are shown in Figure 26. The implants were carefully controlled and were performed at the same dose rate to ensure that the damage versus dose curve can be constructed. The damage as measured by the number of counts at the point of maximum damage is plotted as a function of implant fluence in Figure 27.

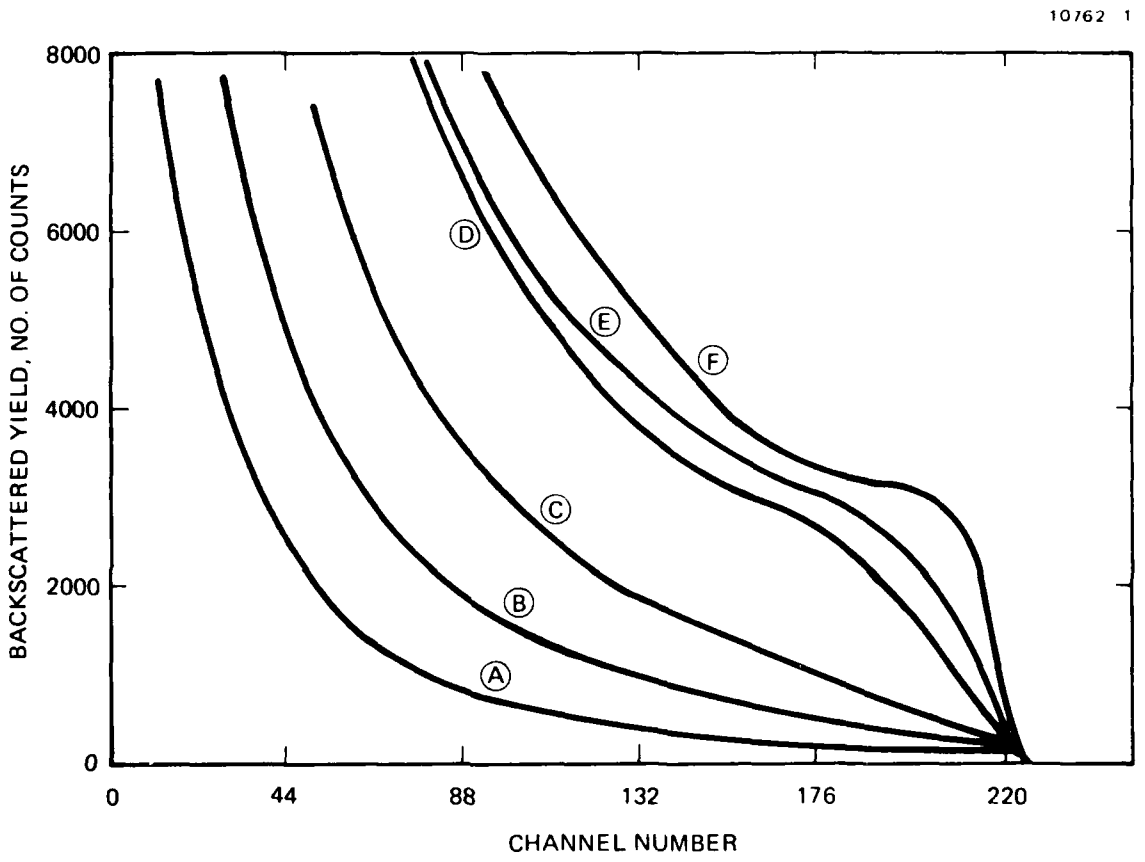

Figure 26. RBS spectra obtained from InP samples.

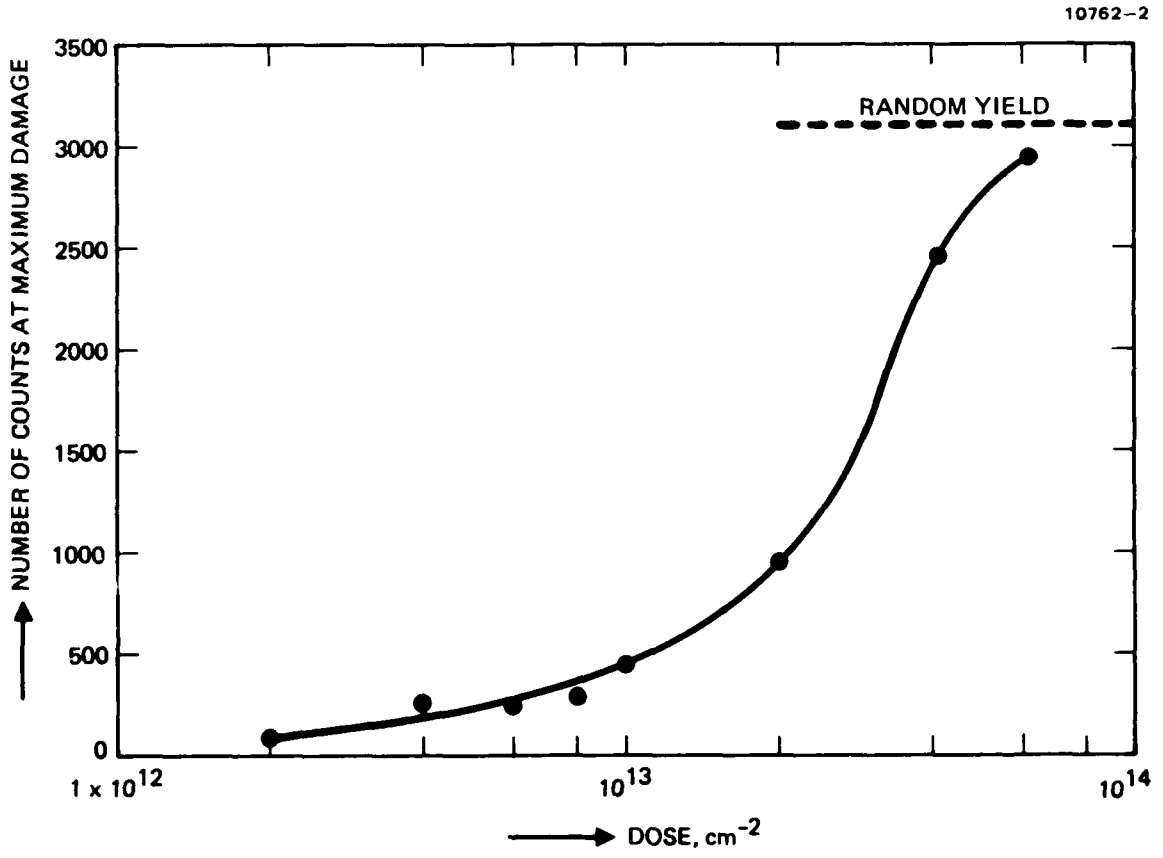

Figure 27. Dose versus damage curve for InP implanted with silicon at room temperature.

We have analyzed Si implanted and annealed InP samples by RBS analysis. Samples annealed at temperatures of 600°C or higher show that the implant damage as measured by RBS, is essentially annealed out. The channeled spectra from un-implanted virgin and implanted, 600°C annealed samples are essentially identical.

F. RAPID THERMAL ANNEALING OF InP

In conventional furnace annealing, the sample to be annealed is introduced into the furnace. It typically takes a few minutes for the sample to reach thermal equilibrium with the furnace. Thus conventional anneals are performed for time periods ranging from 10 to 30 minutes. This prolonged heat treatment at elevated temperatures can result in diffusional broadening of redistribution of ion implanted dopents. It can also result in the redistribution of dopents impurities present in the substrate. Typical example in InP are: (1) the redistribution behavior of Be, (2) the redistribution of Fe in ion implanted and annealed InP

High intensity laser or electron beams (pulsed or C-W scanned) can be used to rapidly ioning the sample to high temperatures. In these cases the energy is typically absorbed in the near surface region of the sample. The heating is, therefore, localized. Experimental results obtained from ion implanted compound semiconductor samples annealed by such transient beam procesing techniques have been disappointing. Such transient heating introduces severe thermal gradients across the sample, resulting in the formation of major slip planes. These defects degrade the electricl properties of the implanted layer.

Some of these short comings can be overcome by using a properly designed annealing system which employs high intensity lamps to bring the samples to the desired anneal temperature. We have investigated the effectiveness of such an annealing technique. These experiments were performed at A.G. Associates,

Palo Alto, California using a HEATPULSE^{TM} system which is commercially available.

The HEATPULSE 210T system consists of an annealing chamber and a dedicated microprocessor. The annealing chamber contains upper and lower banks of high-intensity, tungsten-halogen lamps and water-cooled, reflective walls. A quartz diffuser tube positioned between the lamp banks is heretically sealed to the door with an o-ring. A flat piece of quartz with small pins attached to the door plate holds the wafer and loads it into the annealing chamber. The visible light emitted from the lamps passes through the quartz tube wall and the wafer tray and is absorbed by the wafer.

The banks contain thirteen 1.5 kW lamps. The maximum input power to the lamps is limited at 18 kW. This power is converted to radiant energy and is efficiently absorbed by the wafer to be annealed. A schematic cross-section of the HEATPULSE system and a block diagram are shown in Figure 28.

A small Si-monitoring piece with a theromocouple glued to it is located in the annealing chamber. the thermocouple signal is fed to the controller, enabling closed-loop temperature monitoring and control of the annealed wafer. This type of temperature monitoring has its own problems. The actual sample temperature for InP mostrates may be different from the measured temperature.

The system has provision for introducing appropriate gases. In all cases discussed in this report, the anneals were performed in an ambient of flowing nitrogen.

We have used this system to anneal Be and Si implanted InP samples. In Figure 29 we show a trace of the monitor thermocouple output during an anneal sequence. The anneal temperature is ~ 700°C. The anneal time is defined as the time during which the sample is maintained at the anneal temperature. The microprocesser allows the rise time (t_r) and the full time (t_f) to be independently controlled.

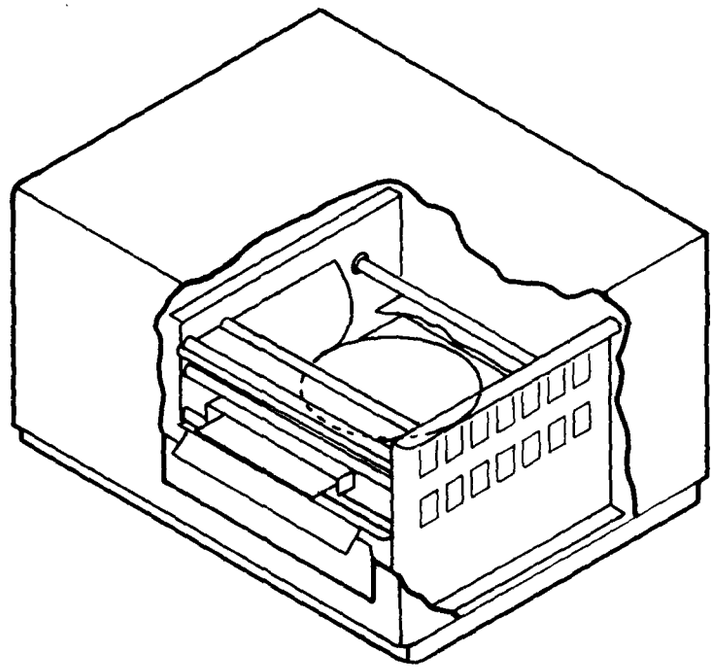

(a) CROSS SECTION

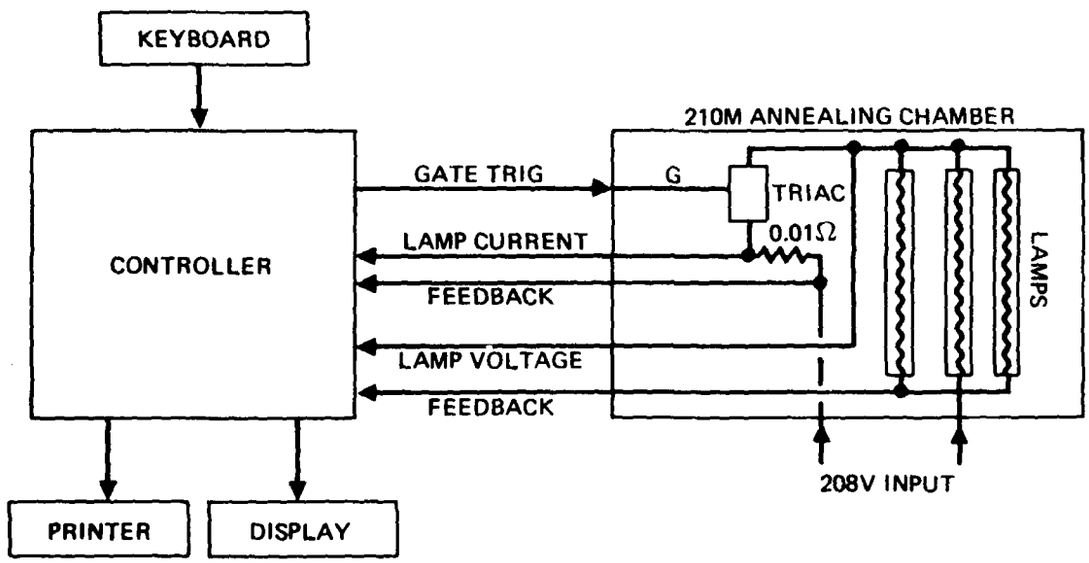

(b) BLOCK DIAGRAM

Figure 28. Schematic diagram of *HEATPULSE 210M* system.

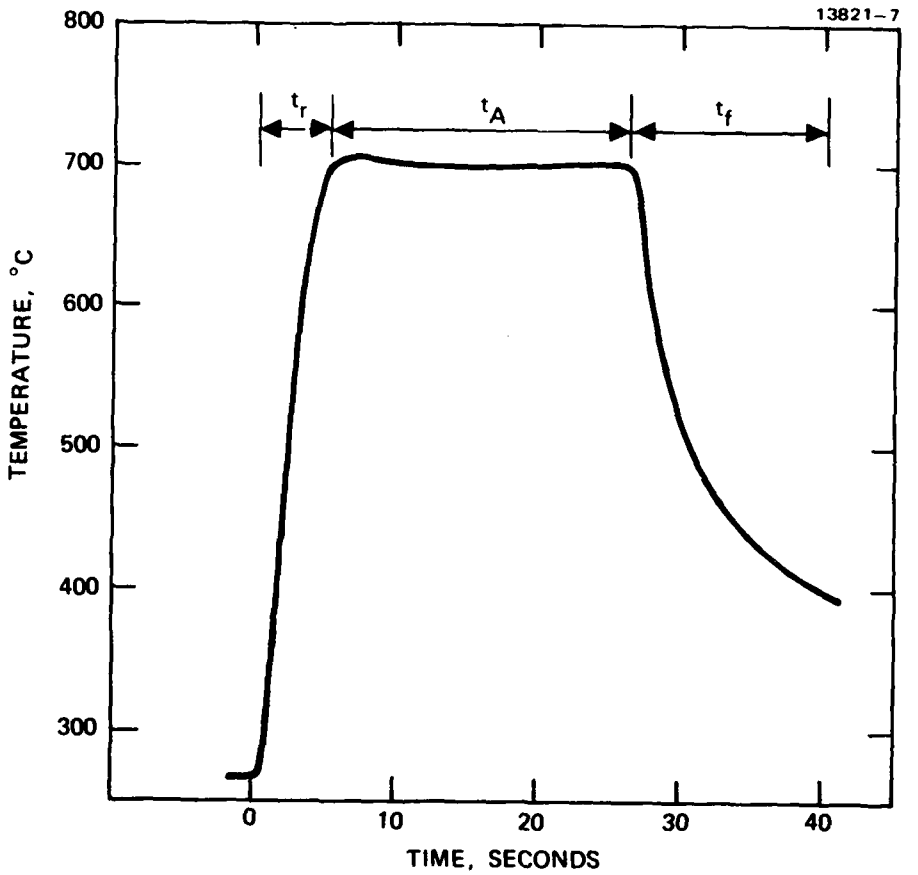

Figure 29. Typical time, temperature curve obtained from a measuring thermocouple in the heat pulse system.

In Figure 30 the electrical properties of Be-implanted and rapid thermally annealed InP samples are presented. The samples were implanted with 200 keV Be ions to doses indicated in the figure. They were encapsulated with 1500 Å of PSG prior to anneal. The anneal temperature was kept at 700°C, and the anneal time was varied from 2 sec. to a maximum of 40 sec. Also shown are results obtained from samples which were furnace-annealed at 700°C for 30 minutes.

As seen from Figure 30, the electrical activation efficiency increases monotonically as the anneal time is increased from 2 sec. to 10 sec. and reaches a maximum value. Prolonged annealing does not increase the doping efficiency.

Figure 31 shows the electrical properties of Si-implanted and annealed InP samples. The samples were encapsulated with PSG and annealed at 750°C. As seen from this figure, the electrical activation efficiency increases monotonically with time for the low fluence implanted ($\sim 1 \times 10^{13}$ cm^{-2}) samples. The mobility recovery is also monotonical. Anneal times of 30 sec. or longer are required to achieve a high degree of electrical activation with acceptable carrier mobilities. In the case of high fluence (1×10^{14} cm^{-2}) implanted samples the carrier activation saturates with ~ 70% activation efficiency for anneal times longer than 20 sec. Again, the mobility recovery is gradual.

The electrical properties of Be- and Si-implanted, rapidly thermally annealed InP show that a high degree of electrical activation with acceptable mobilites can be achieved following anneals for time periods < 1 minute. These preliminary results are extremely encouraging. We will continue to optimize the rapid thermal anneal process and study the redistribution behavior of implanted dopants, as well as thos present in the substrate following rapid thermal annealing as a part of our IR&D program.

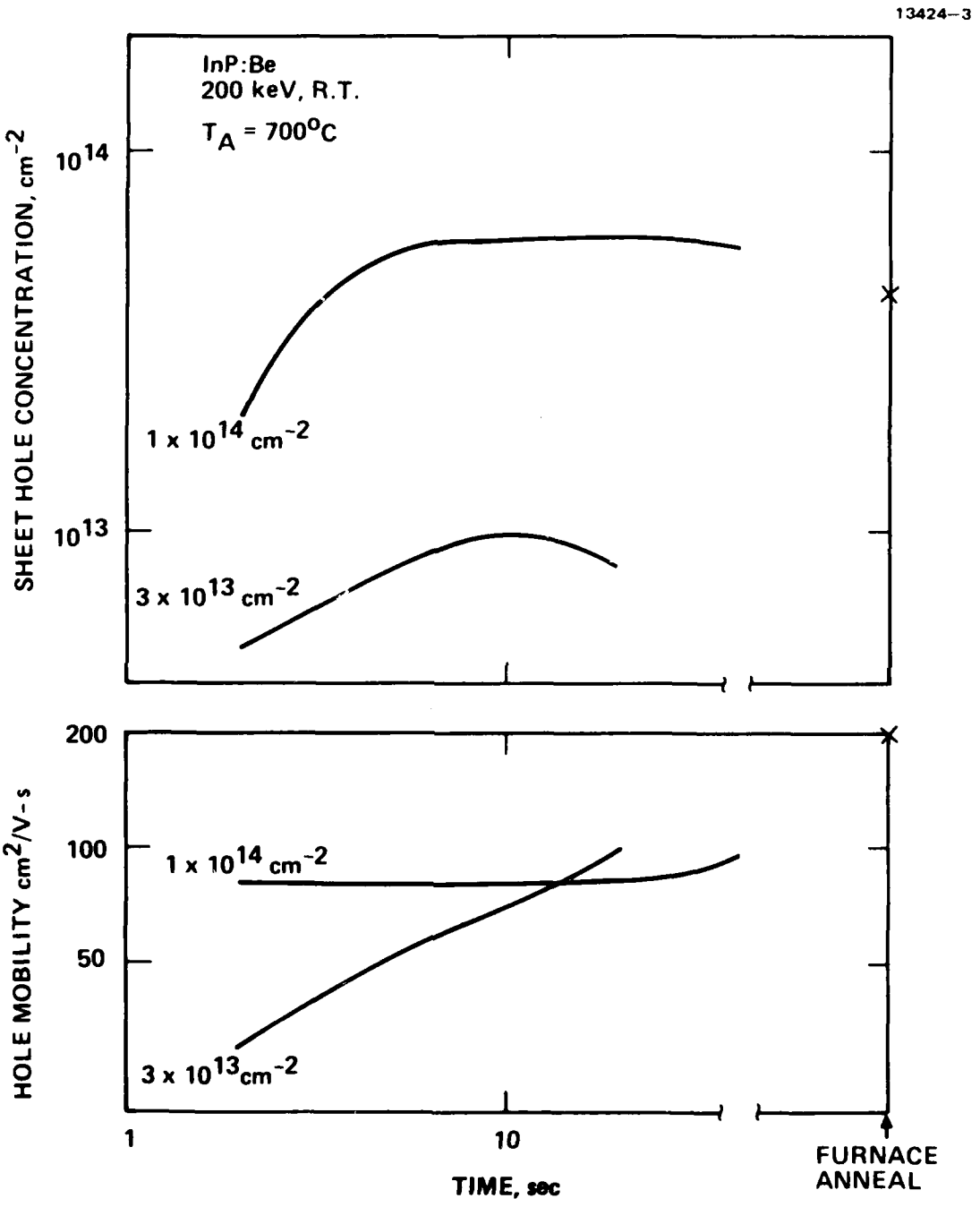

Figure 30. Electrical properties of Be- implanted, rapid thermally annealed InP samples as a function of atom anneal time anneal temperature of 700°C.

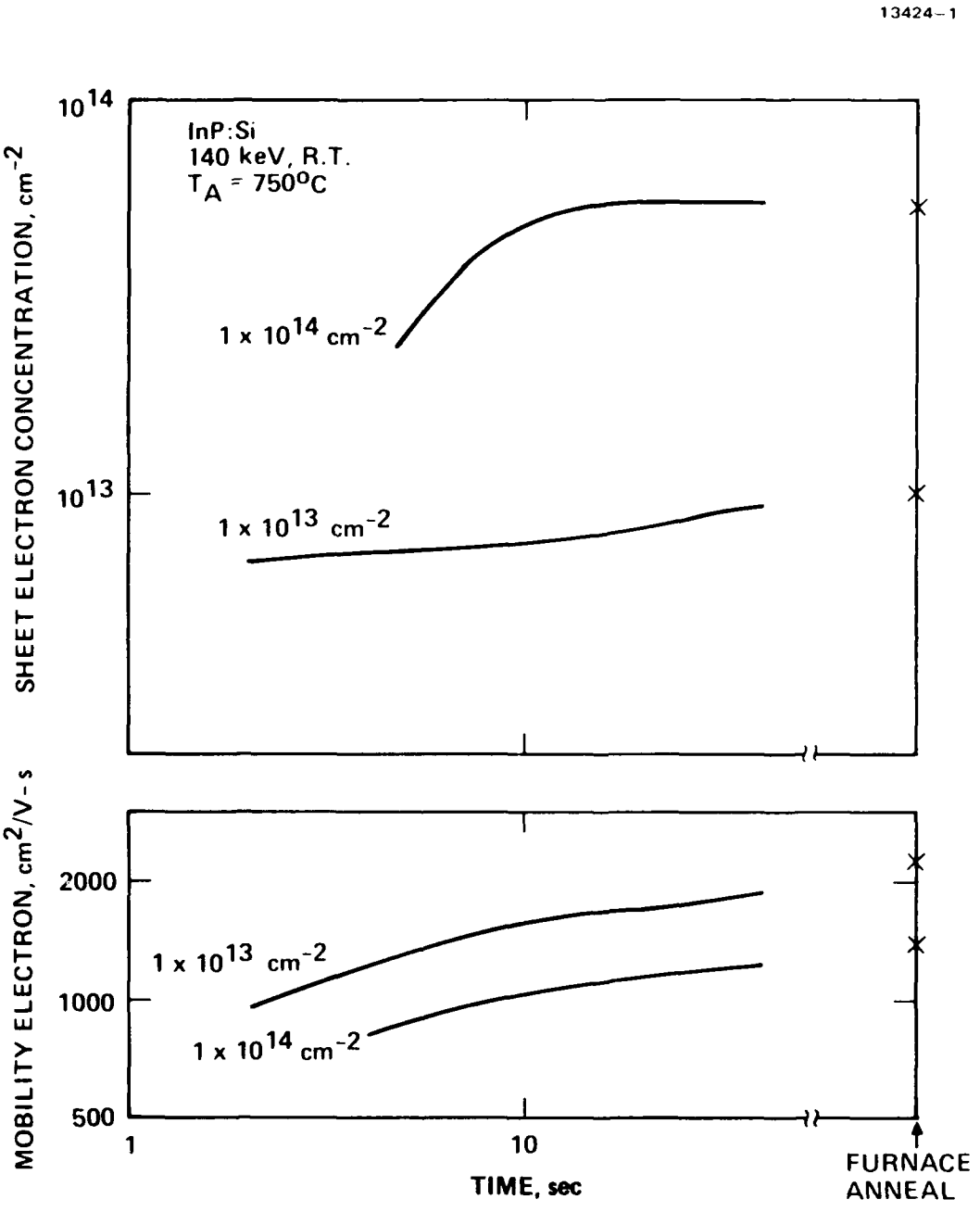

Figure 31. Electrical properties of rapid thermally annealed, Si implanted InP as a function of anneal time at an anneal temperature of 750°C.

G. TRANSMISSION ELECTRON MICROSCOPY (TEM) STUDIES

In this section, we discuss the results obtained from a transmission electron microscopy (TEM) study on ion implanted and annealed InP samples. The TEM measurements were performed at the University of California, Berkeley, under the supervision of Dr. D.K. Sadana and Prof. J. Washburn. A subcontract at a level of $25,000 was issued.

Two different microscopes were used in this study. They were either Philips Model 301 or Philips Model 400. These microscopes operate at 100 keV. TEM measurements require extensive specimen preparation. An extensive effort was devoted to developing specimen preparation techniques. Samples to be prepared were cleaved into 2 mm x 2mm-sized specimens. They were then mounted face down on glass discs with appropriate wax and were mechanically polished to a thickness of ~ 50 μm. They were rinsed, cleaned and were mounted on teflon discs. They were then jet chemically thinned in a solution of 3% Br or Cℓ in methanol. Figure 32 shows schematically the cross section of a thinned sample.

In Figures 33 and 34, TEM plan view micrographs obtained from Be implanted and annealed InP samples are illustrated. The micrograph obtained from a low fluence (1×10^{13} cm^{-2}) Be implanted and annealed (700°C) sample is shown in Figure 33, while Figure 34 was obtained from high fluence (1×10^{14} cm^{-2}) implanted samples annealed under conditions described in the figures. In all cases, the Be dose was insufficient to result in the formation of a continuous amorphous layer. In all the micrographs shown here, dislocation loops can be observed. Their vary in density in the various micrographs. Another common feature is the presence of line defects observable in all cases provided bright field diffraction conditions are used.

As seen from Figure 34, the dislocation loops become smaller with increased anneal temperatures. At the highest anneal temperature used (700°C), another type of defect is

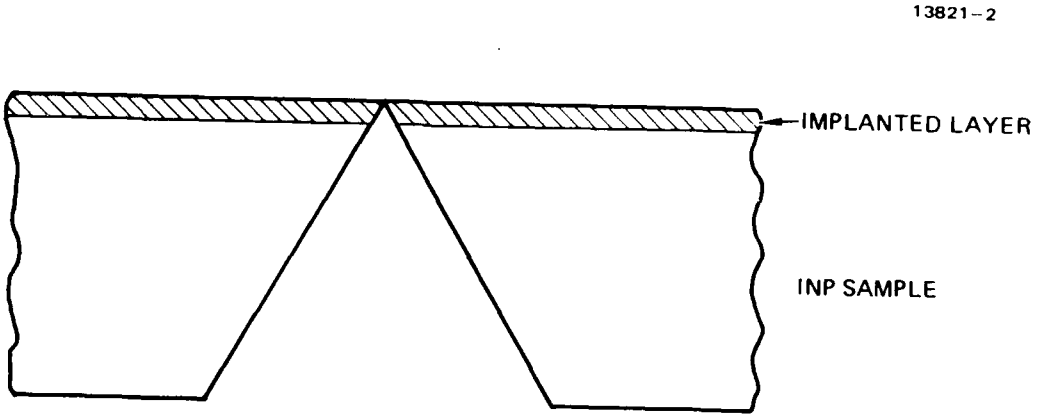

Figure 32. Schematic cross section of a jet thinned InP sample prepared for TEM analysis.

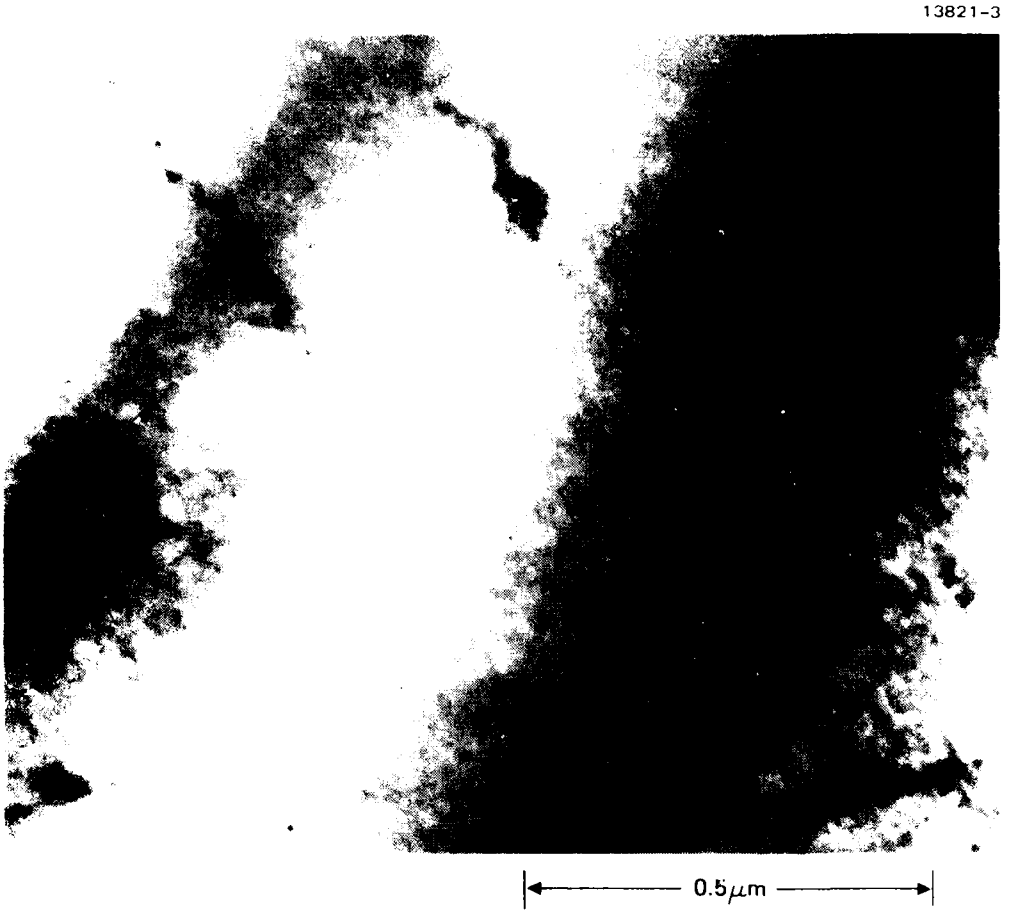

Figure 33. TEM micrograph obtained from a Be-implanted (1×10^{13} cm^{-2}) and 700°C annealed InP sample.

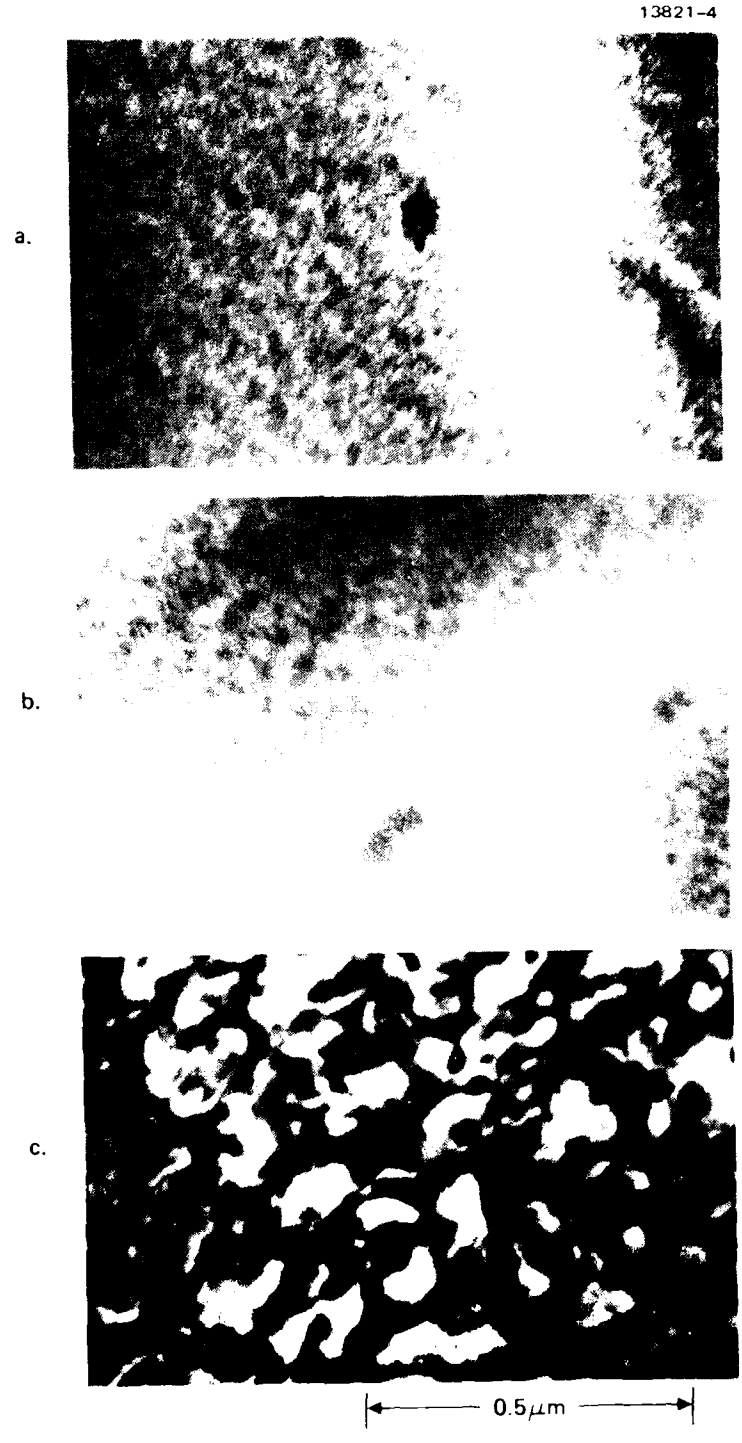

Figure 34. TEM micrograph obtained from a Be-implanted (1×10^{14} cm^{-2}) and annealed InP samples. (a) 650°C anneal, (b) 700°C and (c) 750°C anneal.

observed. It appears that at this temperature severe phosphorus loss may have occurred, resulting in the formation of In-rich precipitates in the near surface region.

In the case of the low fluence Si-implanted sample (1 x 10^{12} cm^{-2}) the 700°C process anneals most of the dislocation loops. The line defects are, however, clearly evident, as seen from Figure 35. The high fluence (1 x 10^{14} cm^{-2}) Si-implanted samples exhibits a continuous amorphous layer in the as implanted state. Annealing at 650°C for 30 minutes results in the formation of a device network of dislocation loops (Figure 36(a)). Annealing at elevated temperatures (700°C and 750°C) reduces these dislocation loops, as seen from Figures 36(b) and (c).

The line defects, in all cases, lie along <100> directions, with preference along one of the two <100> directions. The diffraction contrast of these defects lead us to believe that they are plate like precipitates. From a preliminary analysis of these data, we speculate that these plate-like features represent In precipitates formed as a rsult of P loss during high temperature annealing.

The TEM studies suggest that dislocation loops represent the dominat residual defects in annealed InP. Thermal degradation can occur during high temperature annealing, resulting in loss of phophorus and formation of plate-like defects which maybe In-rich.

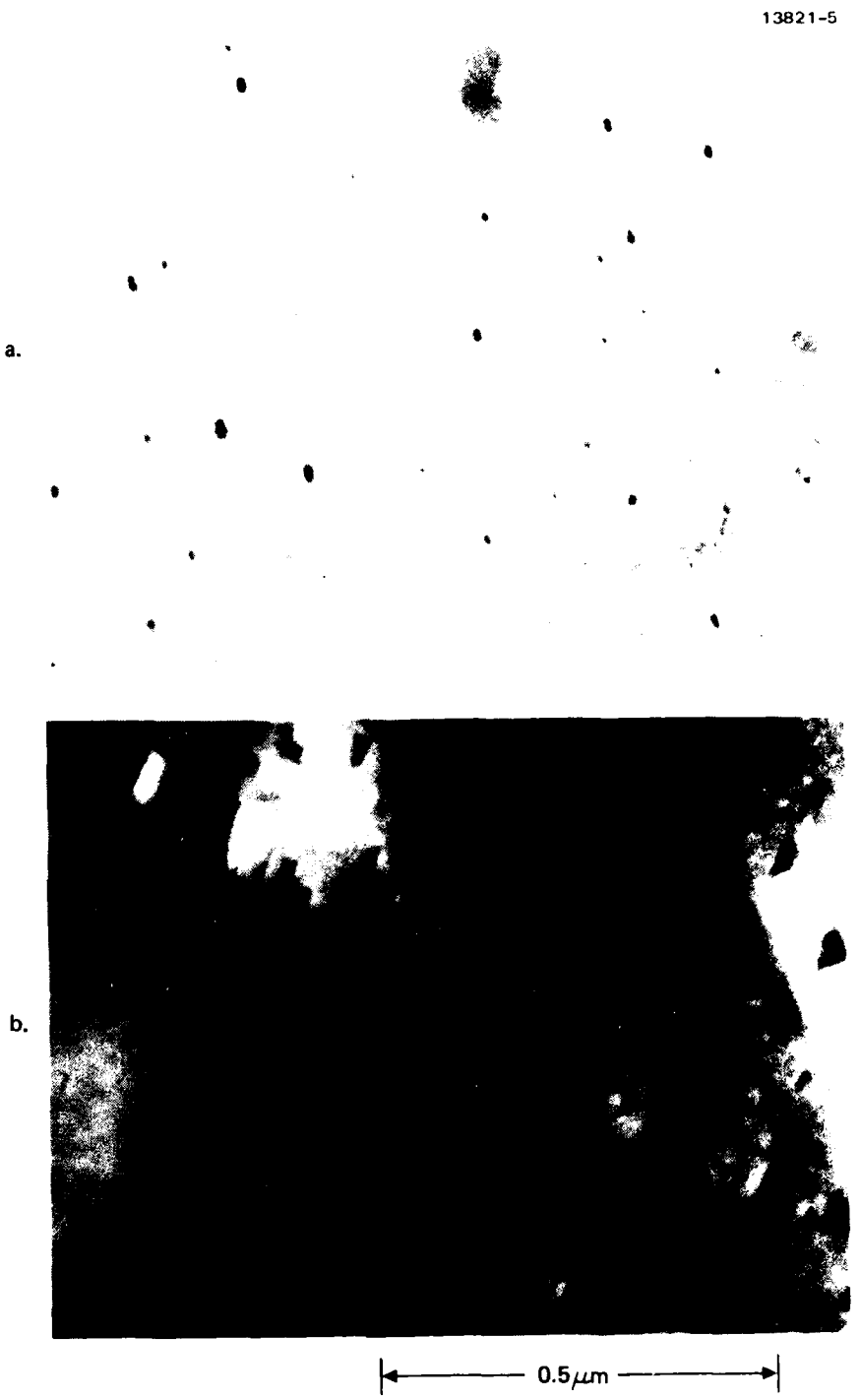

Figure 35. TEM micrograph obtained from a Si-implanted (1×10^{12} cm^{-2}) InP samples. (a) 650°C anneal, (b) 700°C anneal.

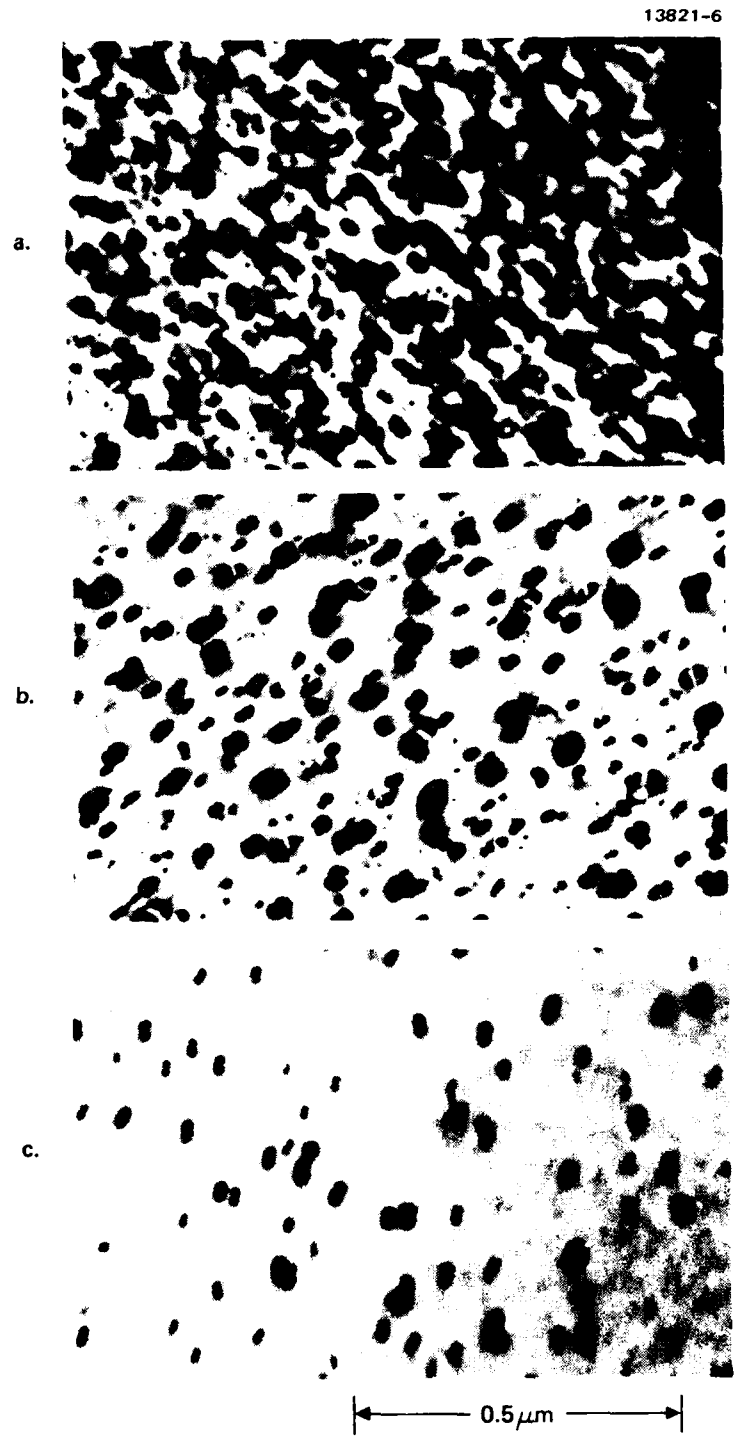

Figure 36. TEM micrograph obtained from a Si-implanted (1×10^{14} cm^{-2}) and annealed InP samples. (a) 650°C anneal, (b) 700°C anneal and (c) 750°C.

SECTION 4

SUMMARY

In this section, we summarize the major conclusions drawn from the present study.

- Annealing of InP for electrical activation of ion implanted dopants requires the development of suitable dielectrics. Candidate dielectrics should be plastic to avoid stressing the sample and also should be rigid to prevent surface degradation. Poorly adhering dielectric encapsulants can result in the loss of phosphorus and in the formation of an In-rich surface layer. Properly deposited phosphosilicate glass (PSG), SiO_2, and plasma-enhanced chemical vapor deposited Si_3N_4 can all act as efficient encapsulants.

- Beryllium is a well-behaved acceptor depant. It can be electrically activated at as low an anneal temperature as 500°C. An acceptably high degree of dopant can be achieved in Be-implanted InP. During high temperature processing, however, dramatic redistribution of implanted Be can take place.

- Silicon, selenium, germanium and tin are well-behaved donor dopants in InP. A high degree of electrical activation can be achieved with these dopants. None of the them diffuse or redistribute significantly during high temperature processing.

- In the case of Se, Ge and Sn, implantation temperature has a significant effect on the electrical activation efficiency. Samples implanted at ~ 150°C show a higher degree of electrical activation than room-temperature-implanted samples.

- Quantitative determination of the concentration of Fe in semi-insulating is a major problem. SIMS, ZAA and EPR were used to determine the concentration of iron in several InP samples. Extreme care is required to determine the concentration of Fe in InP unambiguously.

- Redistribution of iron in semi-insulating InP during high temperature processing is a major problem.

- Annealing at temperatures of 650°C or higher restores the ion implanted, amorphized InP surface to its original surface condition.

- TEM studies show that the residual defects in ion implanted and annealed InP consist primarily of dislocation loops and line defects.